Experimental Use of High-Strength Reinforcing Steel

by

Jere G. Newton
formerly
Associate Designing Engineer

and

Larry G. Walker
Supervising Design Engineer

Research Report Number 25-1 F

Experimental Use of High-Strength Reinforcing Steel
Research Project 1-5-62-25

Conducted by

Bridge Division
The Texas Highway Department
In Cooperation with the
U. S. Department of Transportation
Federal Highway Administration
Bureau of Public Roads

May 1967

The opinions, findings, and conclusions expressed in this publication are those of the authors and not necessarily those of the Bureau of Public Roads.

ACKNOWLEDGEMENTS

The design and test of phases of this experimental project were supervised by Mr. E. L. Hardeman, Senior Bridge Engineer for District 9. Mr. W. R. Casbeer designed the experimental structure and Mr. J. N. Newton was responsible for field tests and data analysis. The research reported was performed in cooperation with the Bureau of Public Roads.

The valuable assistance and cooperation of the Bureau of Public Roads in planning and executing the field tests is greatly appreciated, particularly the work of Mr. R. F. Varney and Mr. C. F. Galambos who were in charge of live load testing and equipment.

TABLE OF CONTENTS

LIST OF FIGURES AND TABLES

LIST OF FIGURES AND TABLES

LIST OF FIGURES AND TABLES

A B S T R A C T

The design, construction and study of a full scale experimental overpass structure is reported.

A-432 reinforcing steel having a minimum yield strength of 60,000 psi was used in the four span (55'-88'-88'-55') continuous haunched concrete girder unit. Ultimate strength theory was used in the design, and stresses were also checked by elastic methods.

Electrical strain gages were installed at selected points on the reinforcing steel and deflection gages employing electrical strain gages were mounted on the completed structure. Oscillographic records of strain and deflection were taken for a series of live load tests.

A three axle truck was used in the live load tests. Speed and lane position were varied for purposes of studying impact, stress distribution, vibration characteristics and deflection characteristics. Comparisons of observed and calculated stresses and deflections were made.

A study of crack width and distribution was made at several times during the test program. Observed crack formation is compared with various crack prediction methods.

Time dependant deflections were observed throughout the test period and compared with deflection predictions.

The performance of the structure appears to be satisfactory. Crack formation is not considered excessive and observed strains indicate an adequate factor of safety against static failure.

Report On

EXPERIMENTAL USE OF HIGH STRENGTH REINFORCING STEEL

I. INTRODUCTION

The successful use of high strength reinforcing steels in Europe and in building construction in this country prompted the Portland Cement Association and other agencies to promote its use in bridges. Laboratory tests have indicated that the high strength steels manufactured in this country would perform satisfactorily under bridge loadings.

In an effort to gain experience in design and construction with high strength steel and to evaluate its performance, the Texas Highway Department initiated plans for a full scale experimental structure. The crossroad structure over Interstate Highway 35 near Hillsboro, Texas, was built as a part of the Interstate Highway Program and the experimental phases of the project were accomplished in a research project in cooperation with the Bureau of Public Roads.

Four structural requirements that must be satisfied by all reinforced concrete bridges have been listed by Fountain

in an unpublished paper (Reference 1). These are:

1. Adequate safety against static failure
2. Adequate safety against fatigue failure
3. Satisfactory crack formation
4. Satisfactory deflections

It is the broad objective of the research reported to evaluate the performance of the experimental structure with respect to these requirements. However, no specific tests were directed toward evaluation of safety against fatigue failure.

II. DETAILS OF THE EXPERIMENTAL STRUCTURE

Description

A four span continuous concrete T-Beam unit having span lengths of 55'-88'-88'-55' was chosen for this study. The 6½" thick slab was cast monolithically with the parabolic haunched girders. Three 2'-4½" wide girders supported the 24' roadway. The total girder depth was 2'-3" in the uniform depth sections and increased to 4'-9" over supports. The design loading was H15 for this 30 degree skew structure. A general layout of the structure is shown in Figure 1 and structural details are shown in Figures 2, 3 and 4.

The interior supports consisted of a single 30" round column under each girder. Hinge action between columns and girders was achieved by placing neoprene cushions on the outer edges of the columns and by placing connecting dowels perpendicular to girders at the center of columns. The U-type abutments and the 30" columns were supported on drilled shafts (cast-in-place piles).

Several structures of this type and of conventional design and reinforcing were constructed on the same project. One of these, a four span continuous concrete T-Beam unit having spans of 55'-76'-76'-55', was chosen as a control structure for comparison purposes.

Material

High Strength A432 reinforcing steel with a minimum yield point of 60,000 psi was chosen for the main steel in the girders and deck slab. Regular strength A15 reinforcing was used for stirrups and for column reinforcing. Concrete with a minimum compressive strength of 3,000 psi and a minimum cement content of 5 sacks per cubic yard was specified.

Design

The continuous girder unit was designed by ultimate strength theory. Load factors of 1.5 for dead load and 2.5 for live load were used except in the cases where dead load and live load were of opposite sign. In these cases the dead load factor used was 0.5. Moment distribution was based on gross section moment of inertia. Lateral distribution of wheel loads followed AASHO design criteria.

Comparison designs were made by elastic theory for both 30,000 psi and 20,000 psi working stress for reinforcing steel. Tension steel requirements determined by ultimate strength theory compared closely with those determined by the elastic theory with 30,000 psi working stress. The major difference in reinforcing steel requirements was in compression reinforcement over supports. No compression steel was required by ultimate theory; whereas, 14.62 sq. in. was required

by elastic theory. The conventional percentage of positive moment steel was extended into supports, however. Bars in girders were cut off as indicated by requirements and no bars were bent up.

Ultimate strength theory was used for design of the deck slab but shear stirrups were designed by conventional elastic design methods.

Top girder steel was distributed over the full width of girder flanges. Three different bar sizes were used to satisfy the tension steel requirements over supports (#7 over the first interior support, #8 over the center support and #9 over the third). This was done to evaluate the effect of bar size on crack width. Crack width predictions were computed by several empirical formulas for comparison with observations.

Deflection predictions based on gross moment of inertia were compared with predictions based on transformed moments of inertia. Both methods gave quite similar deflection patterns. The value of modulus of elasticity normally used in determining construction camber for this type structure is 1.5×10^6. This value was intuitively decreased to 1.0×10^6 for this structure effectively increasing construction camber.

Construction

All forming and falsework for the superstructure was completed prior to beginning concrete placement. All superstructure concrete was completed in seven placements during the period June 18-June 28, 1963, and all forms were released on July 8, 1963. The sequence of placement is shown on Figure 2. Deck placements were finished by longitudinal screeding. The average 28-day compressive concrete strength was greater than 5,000 psi.

III. FIELD TESTS AND EVALUATIONS

Instrumentation

Electrical Strain Gages were bonded to selected reinforcing bars prior to their placement in the forms. The gages used in this test were Baldwin-Lima Hamilton A5-1S6, FAP-50-12-S6, AS-9 and ES-9S gages. The A-5 and FAP-50 gages were temperature compensated for steel; the ES-9S gages were temperature compensated for concrete. The gages were mounted on bars ranging from #4 through #11 with the ES-9S gages placed directly in concrete.

The bars were prepared by grinding the deformations off of half the circumference of the bar for a length of four to six inches. This area was then filed to remove surface irregularities. Acetone was used to remove dirt and grease.

An epoxy and adhesive, formulated by the Texas Highway Department Laboratories, was used to bond the gages to the bars. This was a two component epoxy which was proportioned on precise laboratory scales and stored in separate eight ounce cups. The epoxy could then be field mixed with the critical proportions needed for complete hardening.

Care was exercised in the handling of the gages to avoid getting oil from the hands on the gages and breaking the bond. The gage was glued to the bar and worked into place

carefully to avoid air pockets in the epoxy. The epoxy was allowed to cure for 24 to 48 hours.

Four wire, 25 gauge cable was then soldered to the gages using two leads to each gage wire. The ground wire from the cable was soldered to the reinforcing bar to facilitate resistance to ground checks.

Di-jell wax was used to waterproof the gage and the soldered joint. This wax was melted and applied by drops to avoid air pockets.

The cables were epoxied to the reinforcing steel so that forces applied to the cables would not be transmitted to the delicate gage leads. A two component flexible epoxy, also formulated by the Texas Highway Department Laboratories, was applied over the area to protect the gage and soldered connection from mechanical damage.

Figure 5 shows the method of installation and protection of gages. This method of installation did not prove entirely satisfactory in protecting gages from mechanical damage during steel and concrete placement. A number of gages were damaged beyond repair. Also, the majority of the ES-9S gages placed in the concrete were destroyed.

The installation of the strain gages was completed several months before the actual construction of the

superstructure began. The gages were checked prior to the beginning of construction and all bad gages were repaired or replaced.

Lead cables were brought out of the superstructure at the center column of each of the three interior bents. The lead cables were taped to the reinforcing bars to minimize possible damage from pouring and vibration.

Dummy or temperature compensating gages were mounted on 6" sections of reinforcing bars in the same manner as the active gages. Extra coatings of flexible epoxy were applied to the ends of these sections so that no stress would be introduced through end bearing. These gages were then placed as close as possible to their respective active gages so that the temperature effect would be the same for both gages and both lead wires.

The cables were brought down the columns into terminal boxes strapped to the columns. The cables were soldered to banana jacks mounted on a sheet of plexiglass. The ground wires were shunted together to facilitate resistance to ground tests.

Dynamic deflection measurements were accomplished with devices consisting of cantilever arms clamped to the structure and initially deflected by a wire attached to a fixed

ground reference (Figure 6). Four strain gages were attached to the arm to sense changes in deflection of the arm. These assemblies were then calibrated to indicate structure deflections. It was necessary to correct for changes in the stress on the reference wire due to structure movement.

Equipment for dynamic loading and for recording dynamic strains and deflections was furnished and staffed by the Bureau of Public Roads. Loading was accomplished with a three axle truck which was equipped with instrumentation for measuring dynamic axle loads. The physical dimensions of the truck are shown in Figure 7. It could be loaded to approximate either H15-S12 or H20-S16 loading.

The strain recording equipment had a capacity to monitor over 50 strain gages and/or deflection indicators simultaneously. Gage output was amplified to drive light beam galvanometers which produced oscillographic records on light sensitive paper. It was possible to adjust the amplification and thereby control the amplitude of trace movements on the paper. This instrumentation was calibrated periodically.

Dynamic Live Load Tests

The two-lane structure was divided into five test lanes.

Lanes 1 and 5 were along the east and west curbs respectively, with the tires of the truck approximately 8" from the curbs. Lanes 2 and 4 were the regular traffic lanes and Lane 3 was along the centerline of the structure (Figure 1).

The Bureau of Public Roads test truck made 620 test passes over the five test lanes, each pass being called a run. During these tests, six different sets of gages were monitored. The runs for each set are referred to as a series.

The loading for each series was constant, either H15-S12 or H20-S16. The speed and lanes were varied in each series. Lanes 1 and 5 were used only for creep speed runs because of their nearness to the curbs.

Test loading was done before the bridge approaches were completed. Test runs were made downhill from north to south over a temporary gravel fill, which appeared to cause excessive bouncing of the truck. Severe impact was induced on 27 of the H20-S16 runs by placing ramps in the wheel paths which elevated each axle and allowed it to drop 2" abruptly. The impact ramps were alternately placed at the centerline of the two middle spans, at the 0.6 point of the first span and over each of the interior bents. Only one location was used during any one run.

Three air hoses were mounted perpendicular to the roadway at the beginning, center and end of the bridge to record truck location on the oscillograph records. An event mark was entered on the record as each axle passed over each hose. These air hoses also actuated a digital time counter which timed the passage of the truck to the nearest 1/1000 of a second.

The lateral displacement of each run from the intended test lane was measured by placing a series of pins at the beginning and end of the intended lane. An arm hanging from the center of the truck tripped one of the pins as the truck passed indicating lateral position of the truck.

Manual observations that were recorded for each run included time of day, truck speed, test lane, lateral displacement, and calibration data. Digital data reduction equipment was used to transfer selected oscillographic trace readings to punch cards. The oscillographic record rolls could be mounted on the equipment and easily manipulated with the variable speed two directional chart drive. The setting of vertical and horizontal indicators on a desired trace point produced two analog outputs which were automatically converted to digital output and punched on cards along with certain preset identification data. A computer program was

written to scale and convert digital trace readings to stresses or deflections. The program output of stress or deflection included tabulations by test runs and by individual gages.

Dead Load and Time Dependent Deflections

Accurate levels were taken on the deck surface before and after form removal and periodically thereafter to determine initial dead load deflections and time dependent deflections. The tenth points in each span were marked off along five lines: the centerline, one foot from each curb and the top of curb lines. Levels were taken at the same points on each occasion.

Crack Width Measurements

Crack measurement was accomplished by use of a magnifying comparator. This device is a microscopic viewer in which lines of known width can be compared with cracks to determine widths. By this method the crack width could be measured to the nearest .001 inch at the point of measurement. Crack measurements were taken only at points of maximum width. No measurements were made at points where edge spalling of the crack had occurred since this was not considered representative of the crack width below the surface.

The cracks were first marked by tracing each crack with

a felt marker. This trace followed the entire length of the crack and was drawn as close to the crack as possible. This permitted quick location and identification of each crack and also enabled the crack pattern to be photographed. Points of maximum width were then located and marked so that the same point would be measured each time. Measurement of crack lengths was also made and a terminal reference mark used so that crack extension would be readily visible.

The number system used to identify the cracks was subscripted so that primary, secondary and tertiary cracks could be distinguished. Primary cracks were marked before traffic was placed on the bridge but after form release.

Secondary cracks were identified after a series of "shake down" runs with an H15 and H20 truck. This included some runs over the 2" impact ramps. Cracks were then marked and measured at intervals during the test and after the last run had been made.

Cracks were marked and measured on both top and bottom of the slab in the negative moment area and on the bottom of the girder in the positive moment area.

IV. DISCUSSION OF RESULTS

Dynamic Live Load Tests

Reinforcing Steel Stress. Significant results of live load stress measurements are summarized in Tables 1 and 2. Typical lateral distribution of stress level is shown in Figures 8 through 11. The combination of stresses (Figure 11) produced by test runs in lanes 2 and 4 most nearly approximates design loading assumptions.

Maximum stresses occurred when the H20-S16 test truck passed over the impact ramps. Even in this case, recorded stresses combined with computed dead load stresses were less than calculated values and less than the 30,000 psi value assumed for elastic design comparison. It should be noted that the skew effect and the high concrete strengths would produce a stiffer structure and that the design assumption of cracked section was undoubtedly not present at all gages.

Deflections. Typical live load deflection measurements are shown in Table 3. The effect of truck position on the peak deflection of each girder is presented in Figures 12 through 17. The computed values shown on these figures were determined by calculating the deflection due to one test truck on one girder and distributing this effect to the

three girders in the average proportion of measured deflections.

The accumulated effect of runs in Lanes 2 and 4 may be seen in Figures 18 and 19. The skew effect and increased concrete strength and modulus of elasticity (Ec observed = 5.5×10^6) contribute to reduction of deflections.

Impact and Vibration Characteristics. Measured impact as indicated in Tables 4 and 5 was in general agreement with values computed by A.A.S.H.O. design criteria although it was highly inconsistent. This inconsistency can be partly attributed to the oscillations of the test truck as it came onto the structure. As was mentioned previously, the approaches had not been completed at the time of testing and a temporary gravel fill was used. The vibration frequency and peak double amplitude of vibration measured on truck axles are presented in Tables 6 and 7.

The impact measurements in Lane 2 were consistently high, which may be due to a rougher riding surface in that area. There was no consistent trend of increased impact with increase of speed. Speed had very little effect on peak deflection, as may be seen in Figures 20 through 25.

No unusual vibration characteristics were revealed by these tests. The forced frequency of vibration of the

structure ranged from 2.50 cps to 3.89 cps, as shown in Table 8. The free vibration frequency was about 3.5 cps for the interior spans.

The damping characteristics of the experimental structure were good. A log decrement of damping ranging from .109 to .147 was observed. These values should be considered as approximate since very low amplitudes were being measured. The values of log decrement of damping given above correspond to percentages of critical damping of 1.73% and 2.33% respectively. This compares to a range of 1.4% to 2.0% observed on the A.A.S.H.O. Road Test (Reference 2) for conventionally reinforced concrete bridges.

Dead Load and Time Dependent Deflections

Deflections observed approximately two years after construction were less than the calculated values used in setting construction camber. The calculated values were intuitively increased as described previously to adjust for reduced reinforcing steel area. The adjusted calculation resulted in a predicted final interior span deflection of 0.234 ft., as compared to an observed value of 0.158 ft. after two years. The observed increase in deflection from April 1964 to June 1965 was 0.047 ft. Observed deflections are presented in Figures 26 and 27.

As in live load tests, high concrete strengths and high modul s of elasticity contributed to reduced deflections, but it would appear that the effect of reduced steel percentage was overestimated in design calculations.

Crack Width Measurements

The crack width study reported here is limited to the negative moment area cracks only. The positive moment area measurements were considered unreliable since the girders were rubbed shortly after form removal. The cracks that did reappear were not considered to be representative of the actual crack pattern.

Observed crack widths were compared with theoretical widths predicted by four crack width formulas. These formulas are given below:

(1) Watstein and Parsons with constants evaluated by Clark (Reference 3)

$$W = 2.27 \times 10^{-8} \frac{h-d}{d} \times \frac{D}{p} \left[f_s - 56.6 \left(\frac{1}{p} + n \right) \right]$$

(2) Revised (1959) European Concrete Committee formula-CEB (Reference 4)

$$W_{max} = \left(4.5 + \frac{0.40}{p_e} \right) D \times \frac{f_s}{K_2}$$

(3) Jonsson, Osterman and Wastlund formula (for pure bonding)

$$W_{max} = K \times D \left[\frac{I_c}{d A_s e_t} \times \frac{f_s}{E_s} \right]^{2/3}$$

(4) Kaar and Mattock formula (Reference 6)

$$W = 0.077 \sqrt[4]{A} \; f_s \times 10^{-6}$$

Where: W = Average crack width (inches)

W_{max} = Maximum crack width (inches)

h = Overall depth (inches)

d = Compressive face to tensile steel (inches)

D = Bar diameter (inches)

$$p = \frac{A_s}{A_c}$$

f_s = calculated steel stress (psi)

$$n = \frac{E_s}{E_c}$$

$$p_e = \frac{A_s}{A_c \text{ (effective)}}$$

A_c (effective) is the concrete surrounding the tensile bars having the same centroid as the tensile bars (usually = 2b x cover)

$K_2 = 47.5 \times 10^6$ for deformed bars

K = 0.23 for plain bars

K = .016 for deformed bars

I_c = Gross concrete moment of Inertia (in^4)

e_t = Distance from the neutral axis to the extreme fiber of the tension face (inches)

$$A = \frac{4D^2}{\pi p_e}$$

The formulas of Watstein and Kaar are for average crack width of the primary cracks, while the other two equations are for the maximum crack width at any point. A factor of 1.5 was used to relate maximum to average values for purposes of comparing the four equations. This factor was observed by Hognestad for steel stresses of 30 to 40 Ksi (Reference 5). The dead load steel stresses here were not in this range but no other data was found to correlate average and maximum crack widths of lower steel stresses.

None of the formulas used gave a consistently reliable picture of the average crack width. The formula of the European Concrete Committee yielded the best values as it consistently predicted wider crack widths than the other formulas (Figures 29 through 31).

The maximum crack widths were also closer to the CEB formula. All formulas, however, gave low predictions of maximum width. This is partly due to the presence of a live load in the loading history of the bridge. None of the formulas provide for the existence of short duration live loads. However, even before the live load was applied, the maximum theoretical widths were exceeded by 20 to 60 percent of the observed cracks.

As can be seen from Figure 28, the formula of the CEB

yielded the lowest error. On the other hand, the formulas of Watstein and Kaar have the lowest standard deviation of error with .00122 and .00124 respectively. This compares to the .00134 and .00138 in standard deviation of errors by CEB and Jonssons' formulas.

Although attempts to predict crack width were not satisfactory, the crack pattern and crack widths observed on the structure indicate satisfactory performance. The maximum crack width observed after two years was .010 in. Only two observations exceeded the European Concrete Committee of .008 in. The average width after two years was .0055 in. Average primary crack widths observed at various times are tabulated below:

Date	Bent 2 (#7 Bars)	Bent 3 (#9 Bars)	Bent 4 (#8 Bars)
August, 1963	.0037	.0033	.0046
September, 1963	.0041	.0038	.0046
April, 1964	.0031	.0032	.0025
June, 1965	.0062	.0053	.0049

The measurements in August 1963 were made before any traffic had been placed on the structure. The measurements in September 1963 were made after all live load testing was completed and the structure was opened to regular traffic.

As may be seen from the tabulation of crack widths above, the use of three different bar sizes did not show a consistent trend as to their ability to control cracking.

Both the August and September 1963 readings yielded smaller average crack widths in the area reinforced with #9 bars. The last set of readings shows the largest crack width to be in the area reinforced with #7 bars.

This is contrary to the performance demonstrated in a number of laboratory tests which indicate that smaller bars are superior in controlling crack widths. The final average crack spacing for primary cracks was 1'-6", 1'-8" and 2'-0" for Bents 2, 3 and 4 respectively. This is also contrary to expectations.

Contributing factors to these discrepancies may include variation in concrete quality and weather conditions, the sequence of form release and the fact that most of the impact runs during live load testing were made on the first two spans. It will also be noticed that the dead load deflection of span 2 is greater than that in span 3 (Figure 27). The fact that forms were left in place longer than usual because of unrelated construction scheduling factors may have influenced crack formation. The concrete strengths were high at the time of form release and this may have helped to reduce crack width.

Observations of the control structure with regular reinforcing steel revealed crack formation quite similar to that on the test structure.

V. CONCLUSIONS

Based on the observations and data collected in this study of a full scale experimental bridge constructed with A-432 reinforcing steel, the following is concluded:

1. Measured live load stresses under overload conditions indicate satisfactory working load performance. The H15 designed structure was subjected to H20-S16 loading over impact ramps without causing excessive stress.
2. Dead and live load deflections were smaller than design predictions. This study indicates that the reduced steel percentage resulting from the use of high strength steel has little effect on deflections in the working load range and that conventional methods of calculating deflection are adequate.
3. Measured impact percentages were generally less than A.A.S.H.O. design specification requirements.
4. Damping characteristics of the structure were good and no unusual vibration characteristics were observed.
5. Observed crack pattern and widths indicate satisfactory performance.
6. Nothing in the observed behavior of this structure

indicates unsatisfactory performance.

7. Cost experience on this project indicates considerable cost advantage in the use of high strength steel in this type structure. An estimated 30 percent reduction in reinforcing steel resulted. Some reduction in concrete quantity was also possible due to being able to reduce width of girder stems. The contractor's unit price bid for A-432 steel was 9.8 cents per pound in place, which was the same as the price for A15 steel. The cost of the structure in place (excluding cost of drilled shafts, riprap, railing and armour joints) was $4.32 per sq. ft. The overall saving for the structure was estimated at 10 percent.

APPENDIX

References

Figures and Tables

REFERENCES

1. Fountain, R. S. "High Strength Reinforcing Steel For Bridges," (Unpublished paper).

2. "Dynamic Studies of Bridges on the A.A.S.H.O. Road Test," Highway Research Board Special Report 71.

3. Clark, Arthur P. "Cracking in Reinforced Concrete Flexural Members." ACI Journal Vol. 27, No. 8 (April 1956).

4. Gaston, J. R. and Hognestad, Eivind. "High Strength Bars As Concrete Reinforcement Part 3. Tests of Full Scale Roof Girder," PCA Journal Vol. 4, No. 2, 10-23 (May 1962).

5. Hognestad, Eivind. "High Strength Bars As Concrete Reinforcement, Part 2. Control of Flexural Cracking," Journal PCA Vol. 4, No. 1, 46-63 (January 1962).

6. Kaar, P. H. and Mattock, A. H. "High Strength Bars As Concrete Reinforcement, Part 4. Control of Cracking." Journal PCA, Vol. 5, No. 1, 15-38 (January 1963).

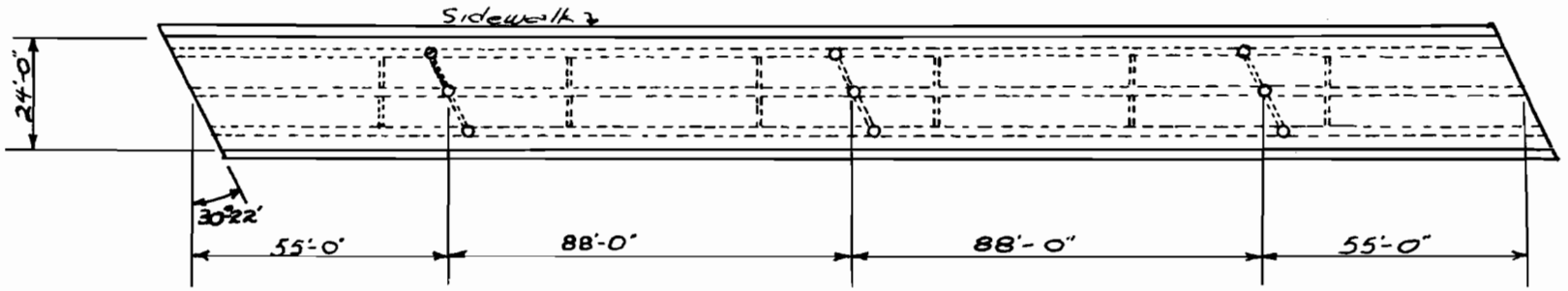

PLAN VIEW

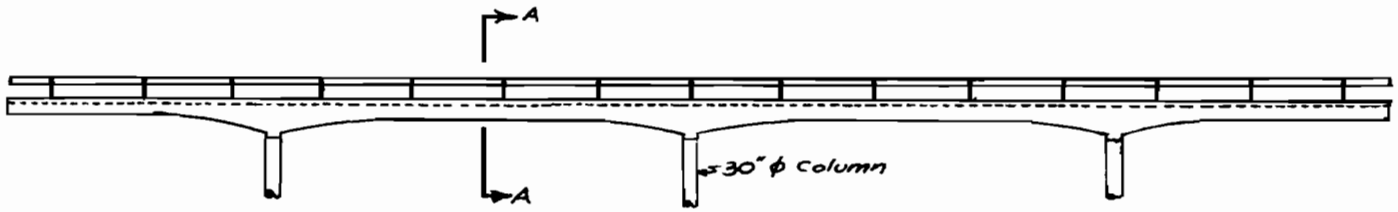

BRIDGE ELEVATION

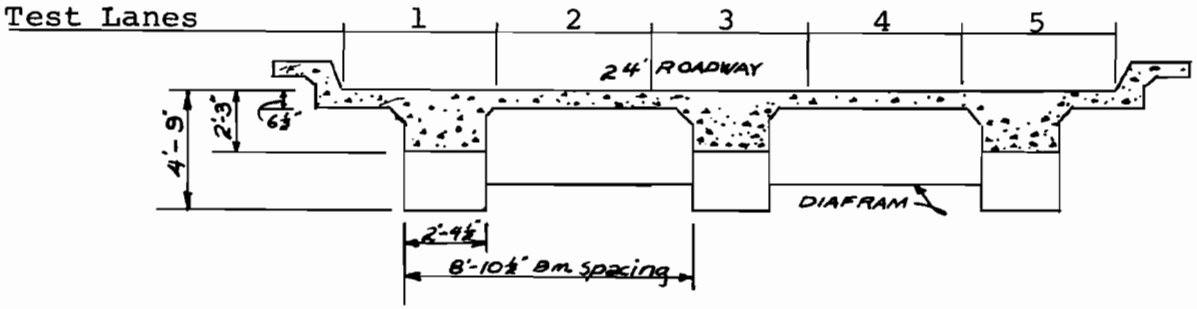

SECTION A-A

Figure 1 STRUCTURE LAYOUT

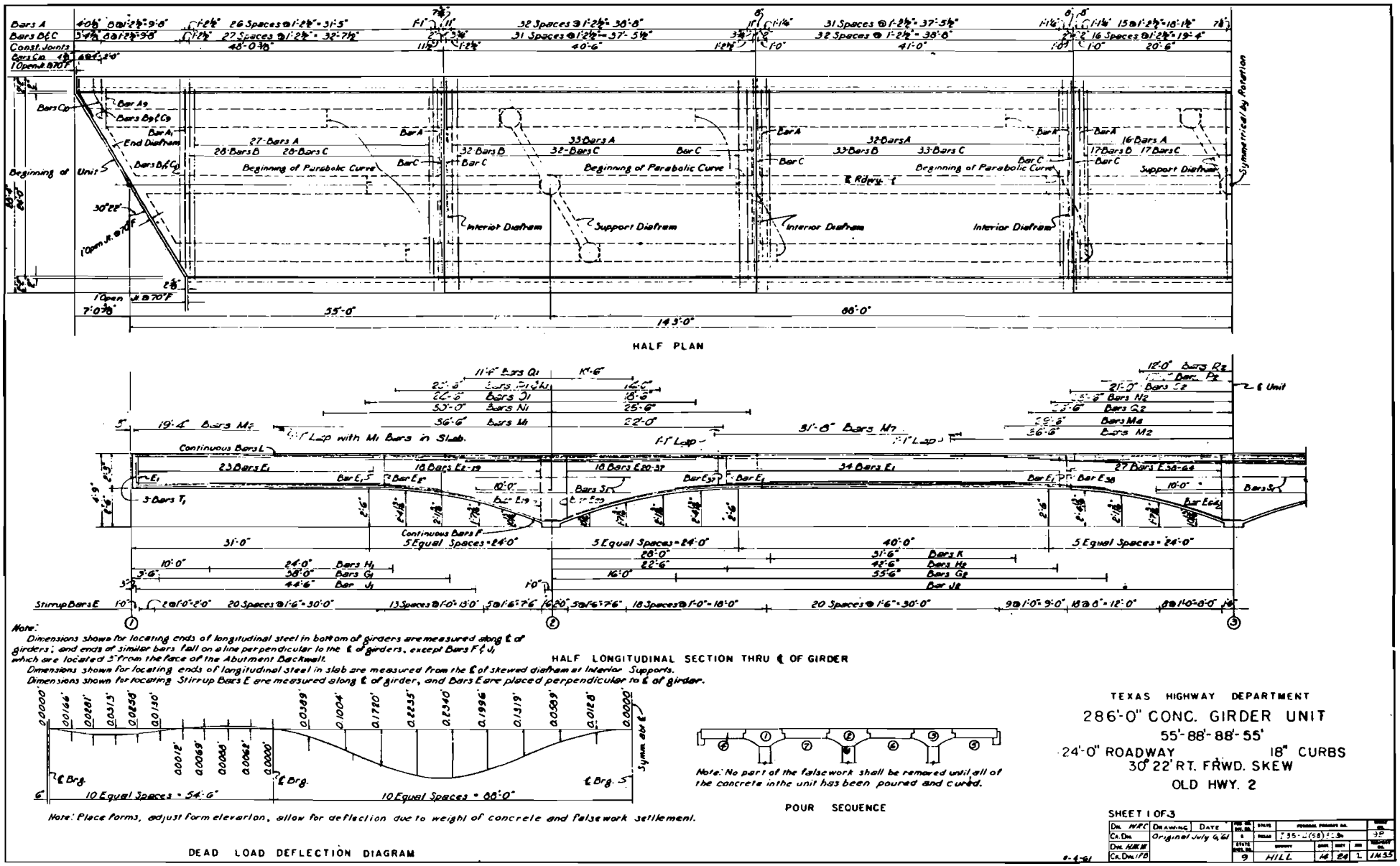

TEXAS HIGHWAY DEPARTMENT

286'-0" CONC. GIRDER UNIT

55'-88'-88'-55'

24'-0" ROADWAY 18" CURBS

30° 22' RT. FRWD. SKEW

OLD HWY. 2

SHEET 1 OF 3

Des. HFC	Drawing	Date
Ck. Des.		Original July 6, 61
Des. HFC W		
Ck. Des. FB		

State	Federal Project No.		
6	F 355-1(58) FC 34		39
State Dist. No.	County	Sect.	Hwy.	Sub
9	HILL	16	28	L

Sheet No. 1M35

8-4-61

Figure 2 STRUCTURE DETAILS

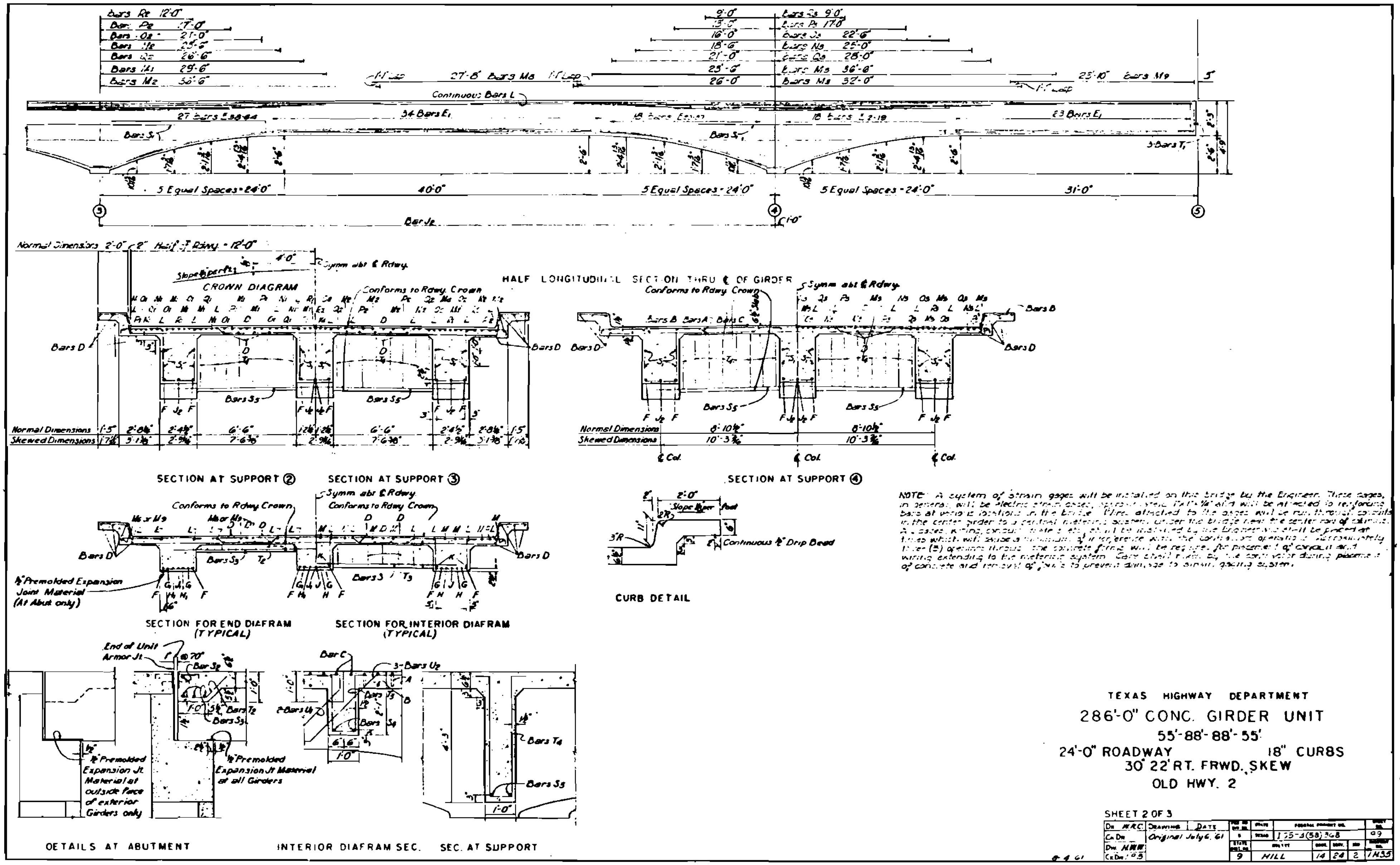

Figure 3 STRUCTURE DETAILS

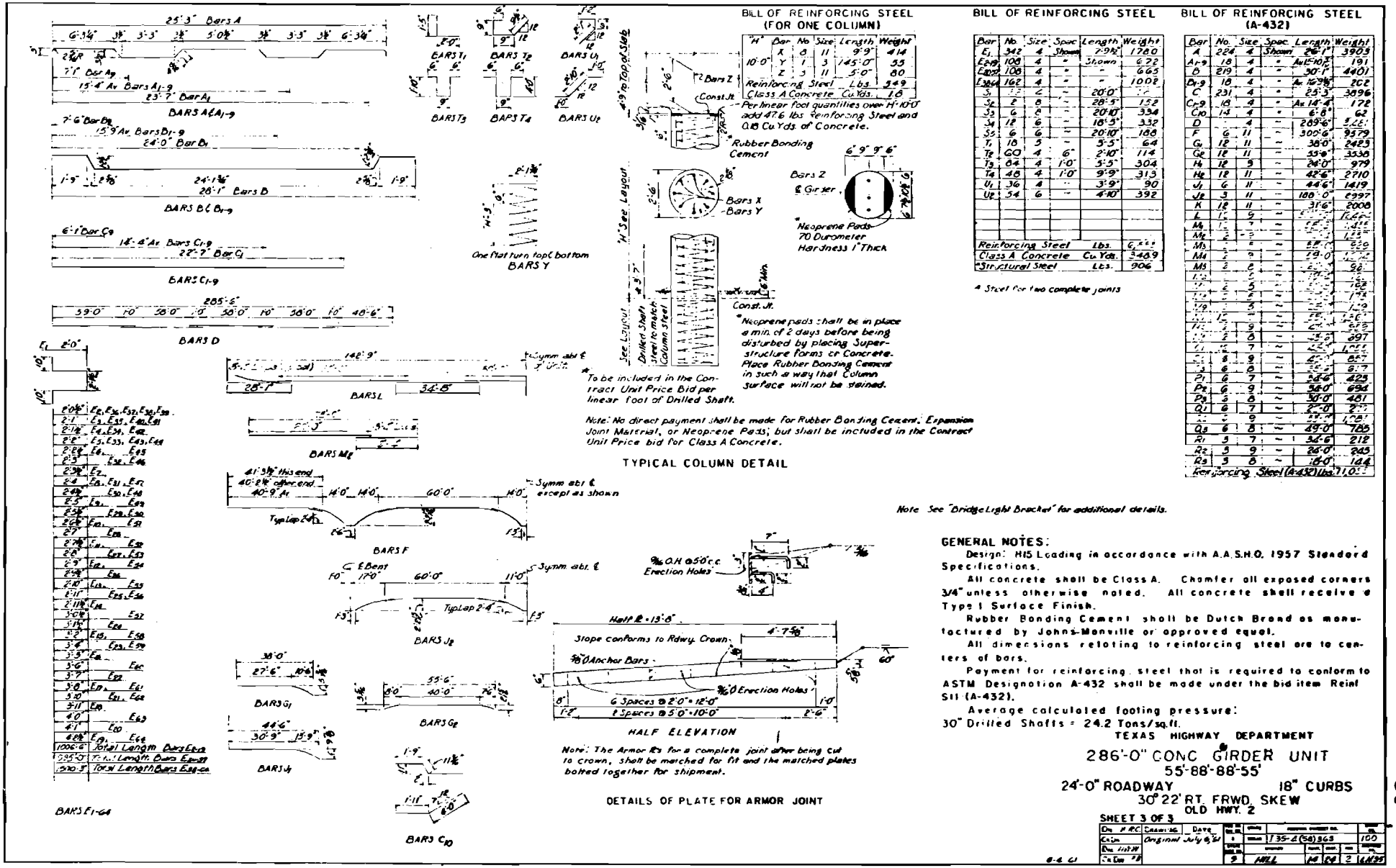

Figure 4 STRUCTURE DETAILS

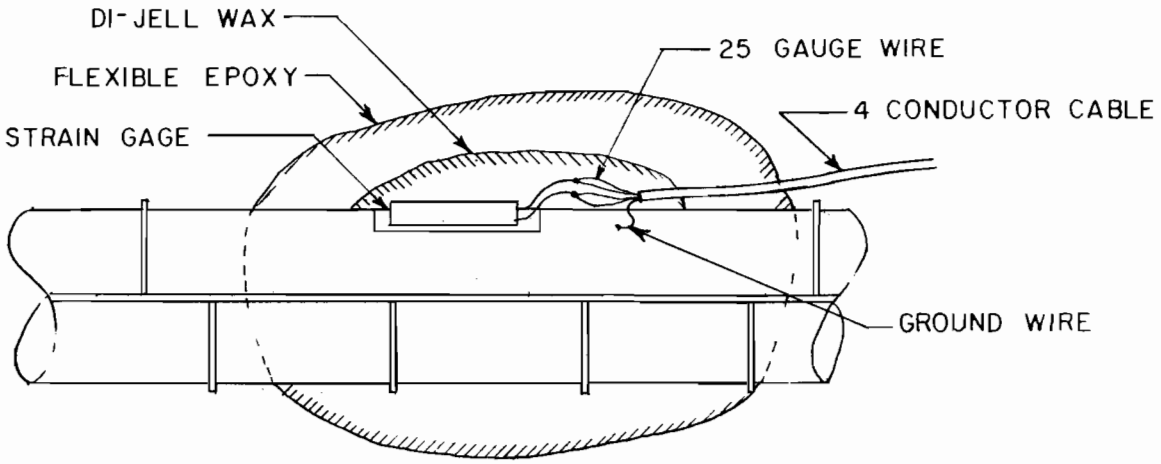

Figure 5 STRAIN GAGE INSTALLATION

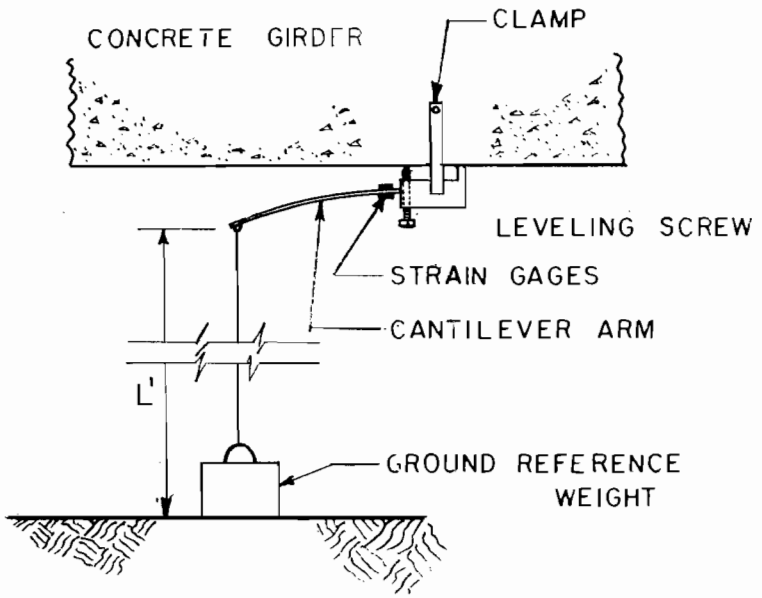

Figure 6 DEFLECTION GAGE

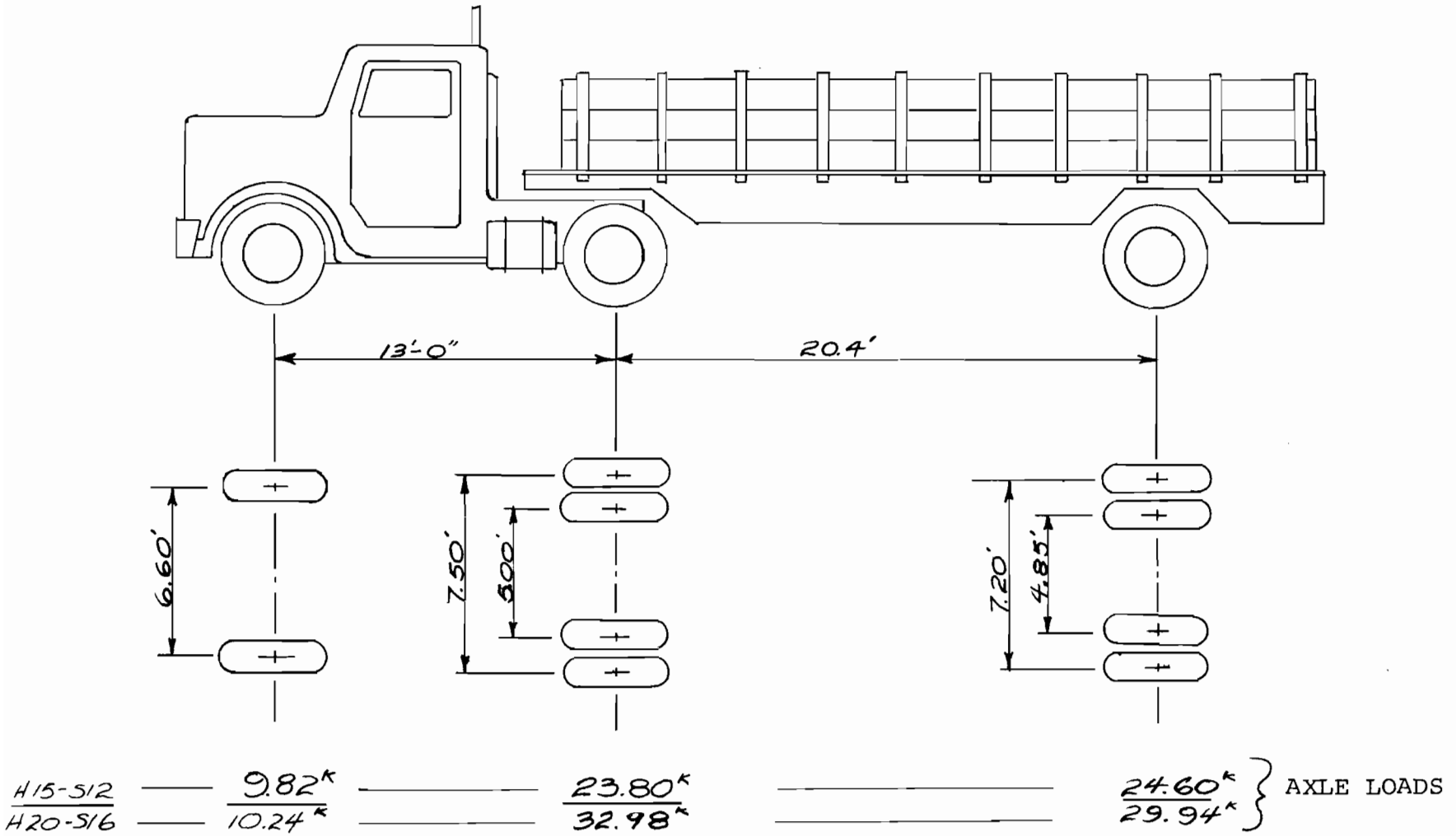

Figure 7 AXLE LOADS AND WHEEL SPACINGS

TABLE 1

STEEL STRESS (PSI) IN BOTTOM OF
GIRDERS CENTER OF SPAN 2

LOADING	SPEED	EAST GIRDER SPAN 2				WEST GIRDER SPAN 2			
		LANE 2	LANE 3	LANE 4	LANE 2 & 4	LANE 2	LANE 3	LANE 4	LANE 2&4
H15-S12	5	2690	1935	1357	4047	-	-	-	-
	10	2868	2151	1056	3924	-	-	-	-
	15	1887	1471	1116	3003	-	-	-	-
	20	1982	1460	1246	3228	-	-	-	-
	25	3217	2398	1781	4998	-	-	-	-
H20-S16	5	3705	2636	1924	5629	2790	3314	4687	7477
	10	3870	2761	2171	6041	2790	3771	4534	7324
	15	3823	2926	2312	6135	2791	3306	4530	7321
	20	4318	3044	2289	6607	2919	3585	4723	7642
	25	4342	3328	2454	6797	-	-	-	-
	IMPACT	5950*	5202*	4169*	10119*	-	-	7074*	-

*Impact boards in center of Span 2

TABLE 2

STEEL STRESS (PSI) IN BOTTOM OF
CENTER GIRDER SPAN 4

LOADING	SPEED	CENTER GIRDER SPAN 4			
		LANE 2	LANE 3	LANE 4	LANE 2 & 4
H15-S12	5	2231	2549	2231	4462
	10	1839	2565	2629	4468
	15	2437	2803	2587	5024
	20	-	-	-	-
	25	2048	2402	2200	4248
H20-S16	5	2961	3435	3125	6086
	10	2879	3428	3195	6074
	15	3112	3528	3478	6590
	20	2746	3428	2979	5725
	25	2845	3528	3211	6056
	IMPACT	-	-	-	

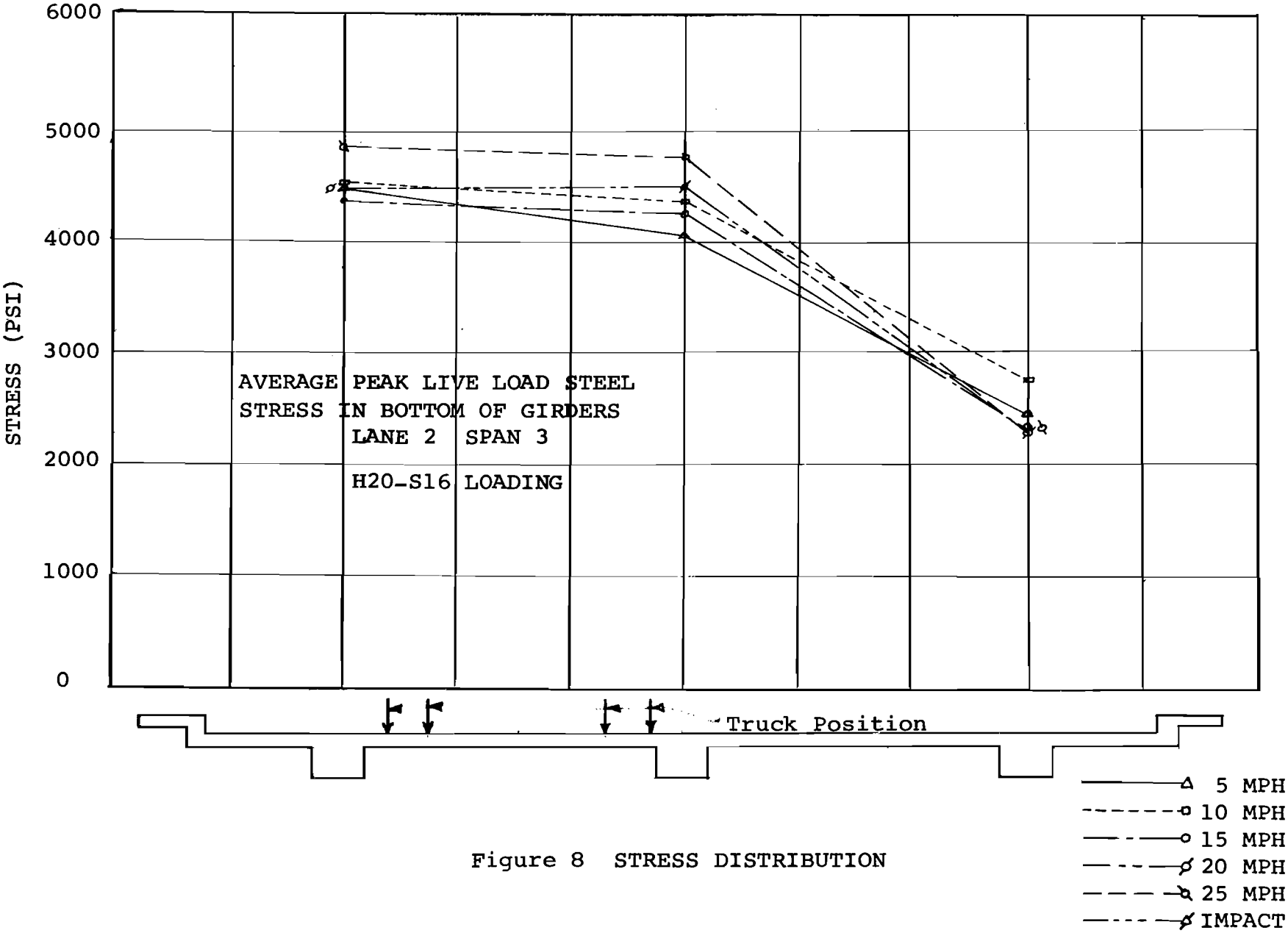

Figure 8 STRESS DISTRIBUTION

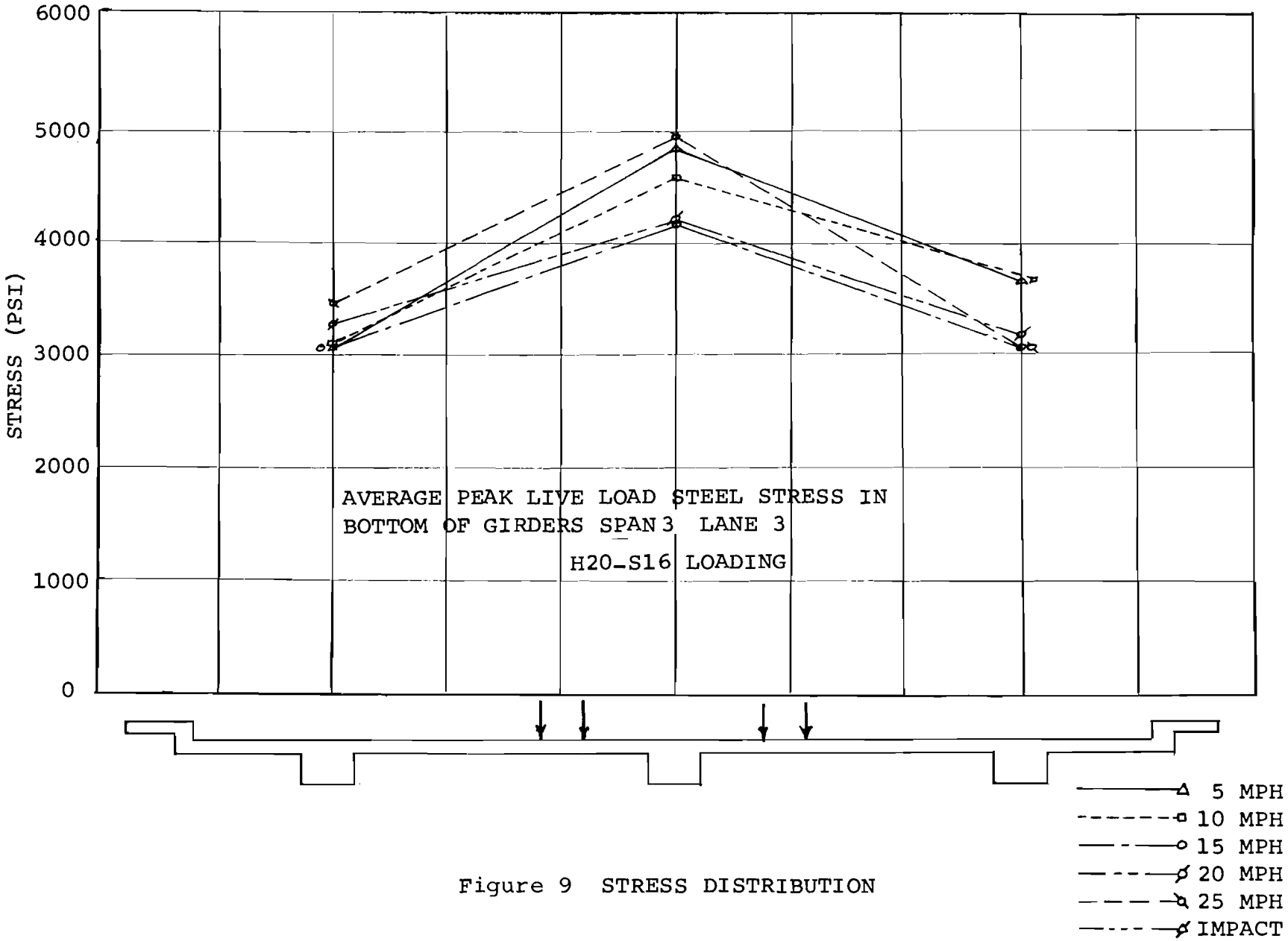

Figure 9 STRESS DISTRIBUTION

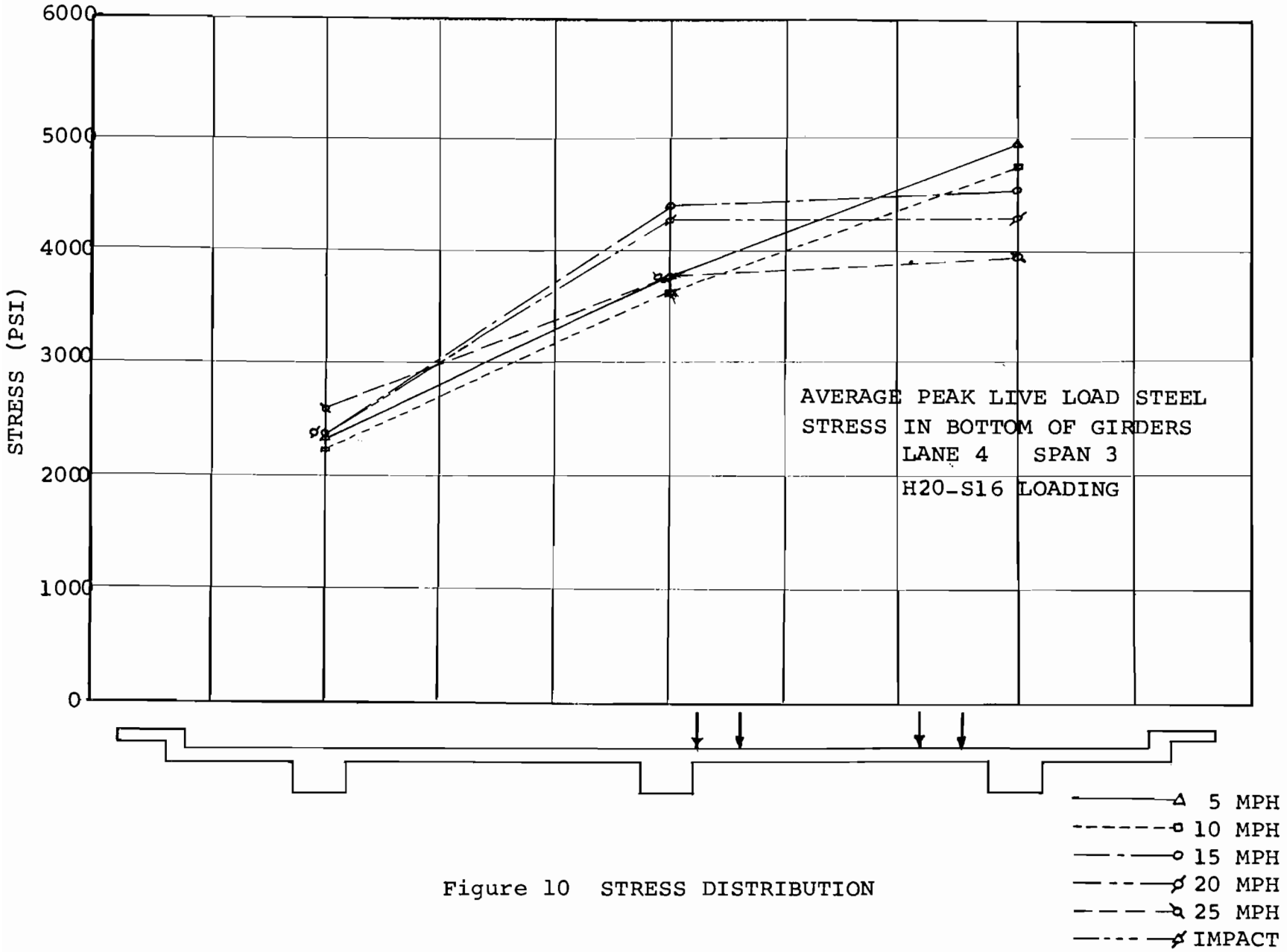

Figure 10 STRESS DISTRIBUTION

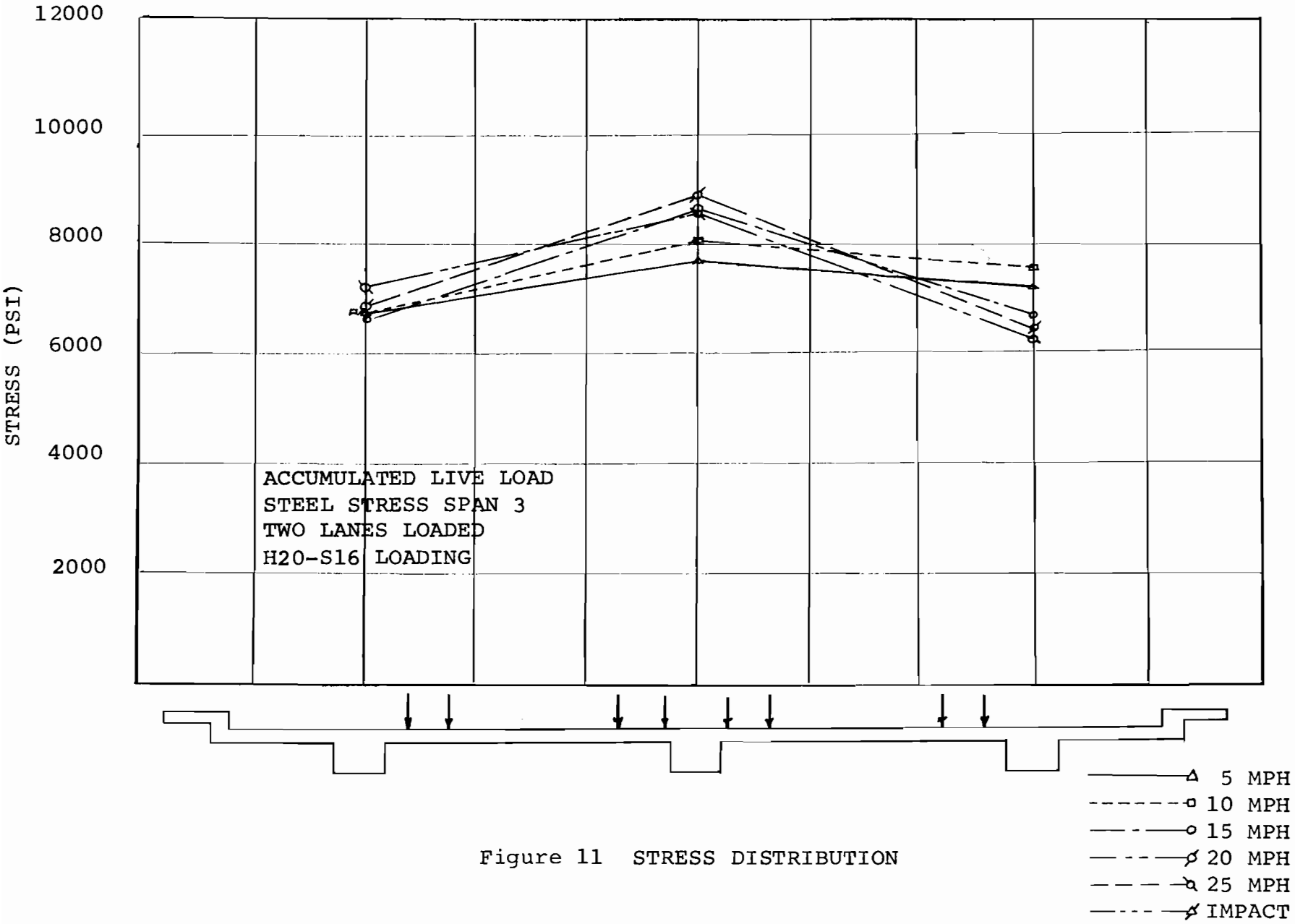

Figure 11 STRESS DISTRIBUTION

TABLE 3

DEFLECTION OF CENTER GIRDER (INCHES)

LOADING	SPEED	Span 3				Span 4			
		LANE 2	LANE 3	LANE 4	LANE 2 + 4	LANE 2	LANE 3	LANE 4	LANE 2 + 4
H15-S12	5	.248	.257	.265	.513	.086	.096	.087	.173
	10	.302	.360	.360	.662	.092	.099	.099	.191
	15	.295	.289	.282	.577	.097	.110	.104	.201
	20	-	-	-		.090	.092	.113	.203
	25	.300	.302	.287	.587	.094	.099	.101	.195
H20-S16	5	.356	.372	.363	.719	-	-	-	
	10	.395	.386	.369	.764	-	-	-	
	15	.376	.385	.382	.758	.141	.174	.147	.288
	20	.399	.392	.389	.788	.136	.162	.149	.285
	25	.362	.382	.395	.767	.147	.110	.111	.258
	Impact	-.808*	-.816*	-.743*	-1.551	-	-	-	

*Impact boards in center of span 2

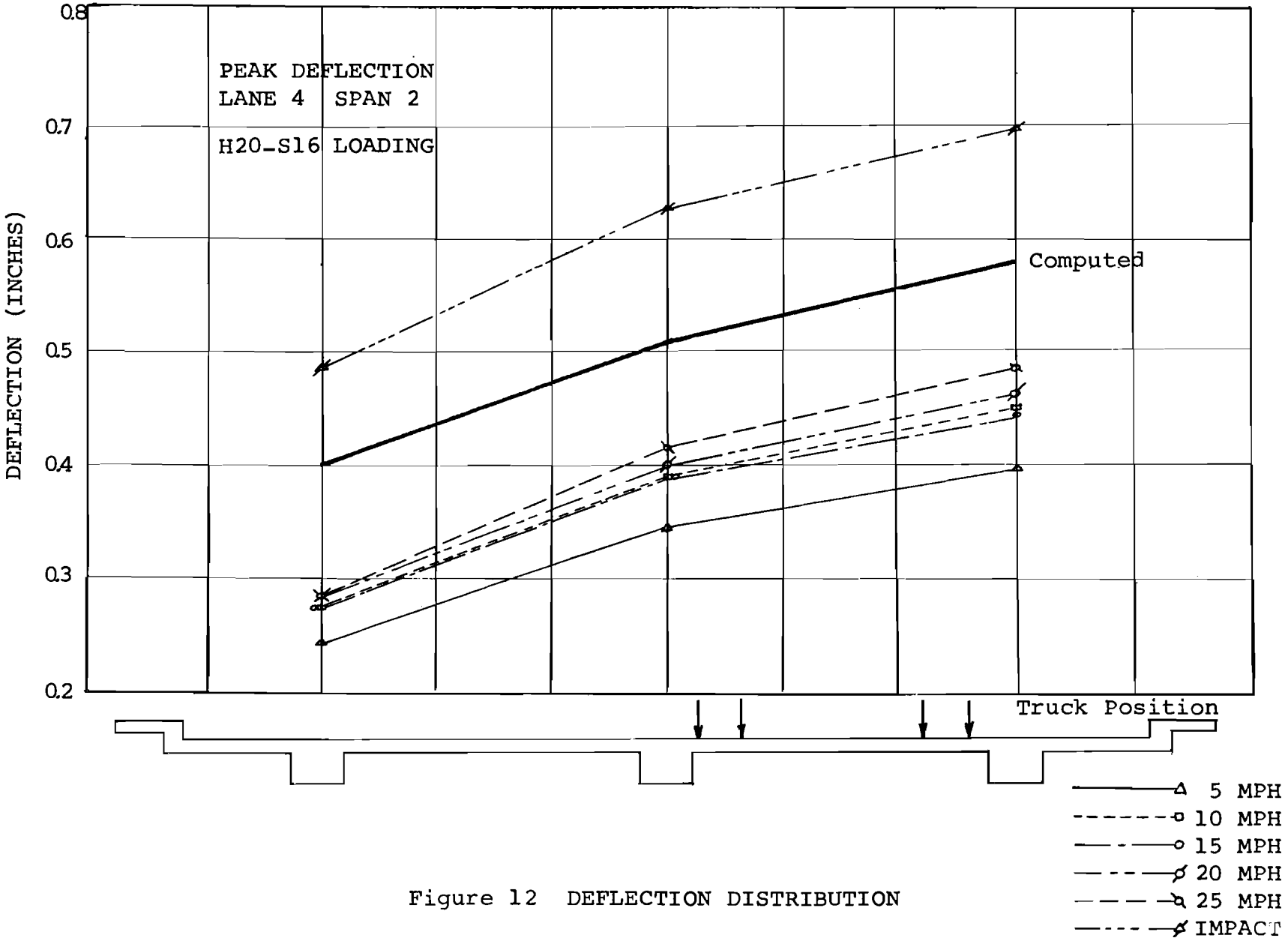

Figure 12 DEFLECTION DISTRIBUTION

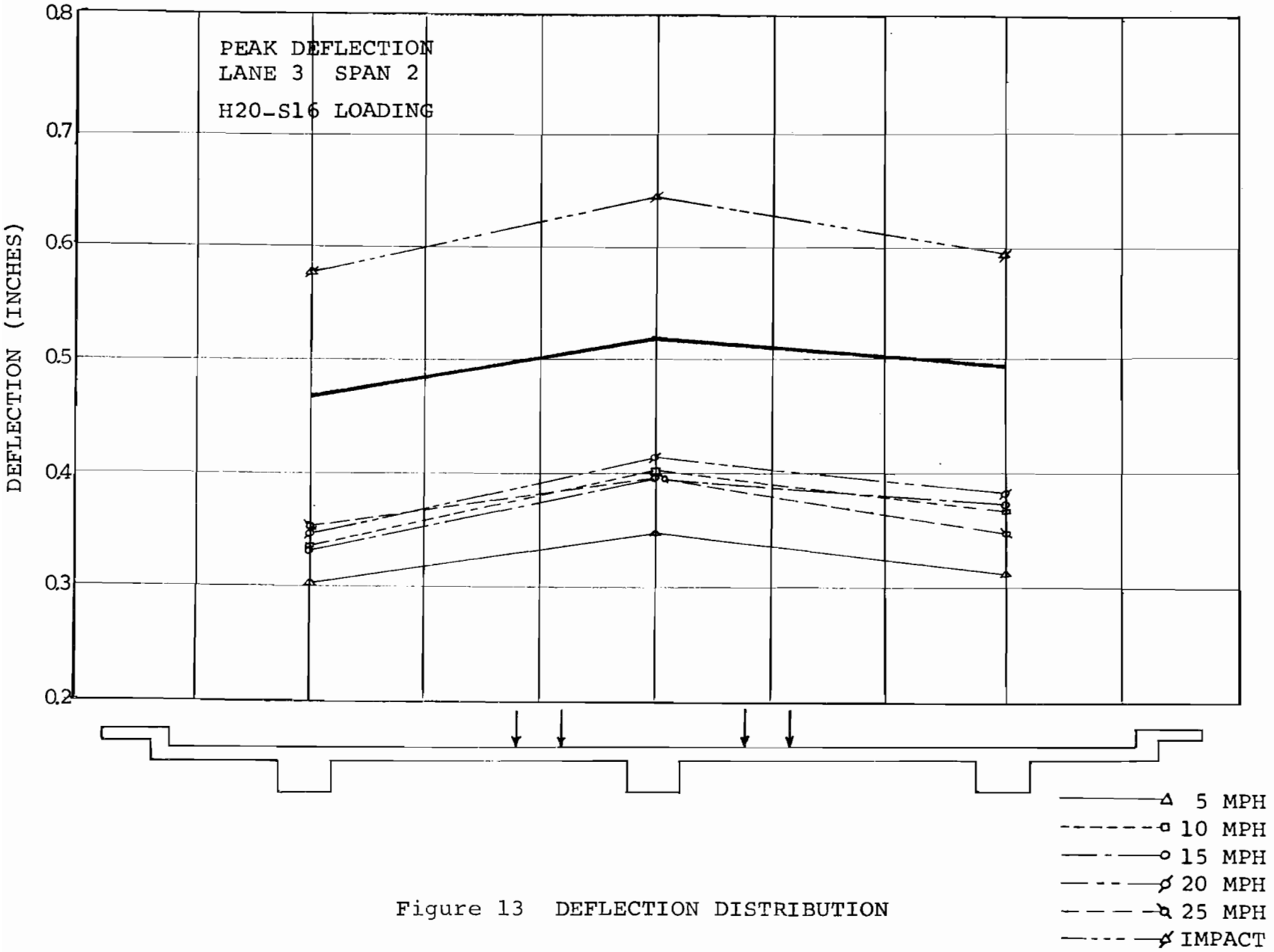

Figure 13 DEFLECTION DISTRIBUTION

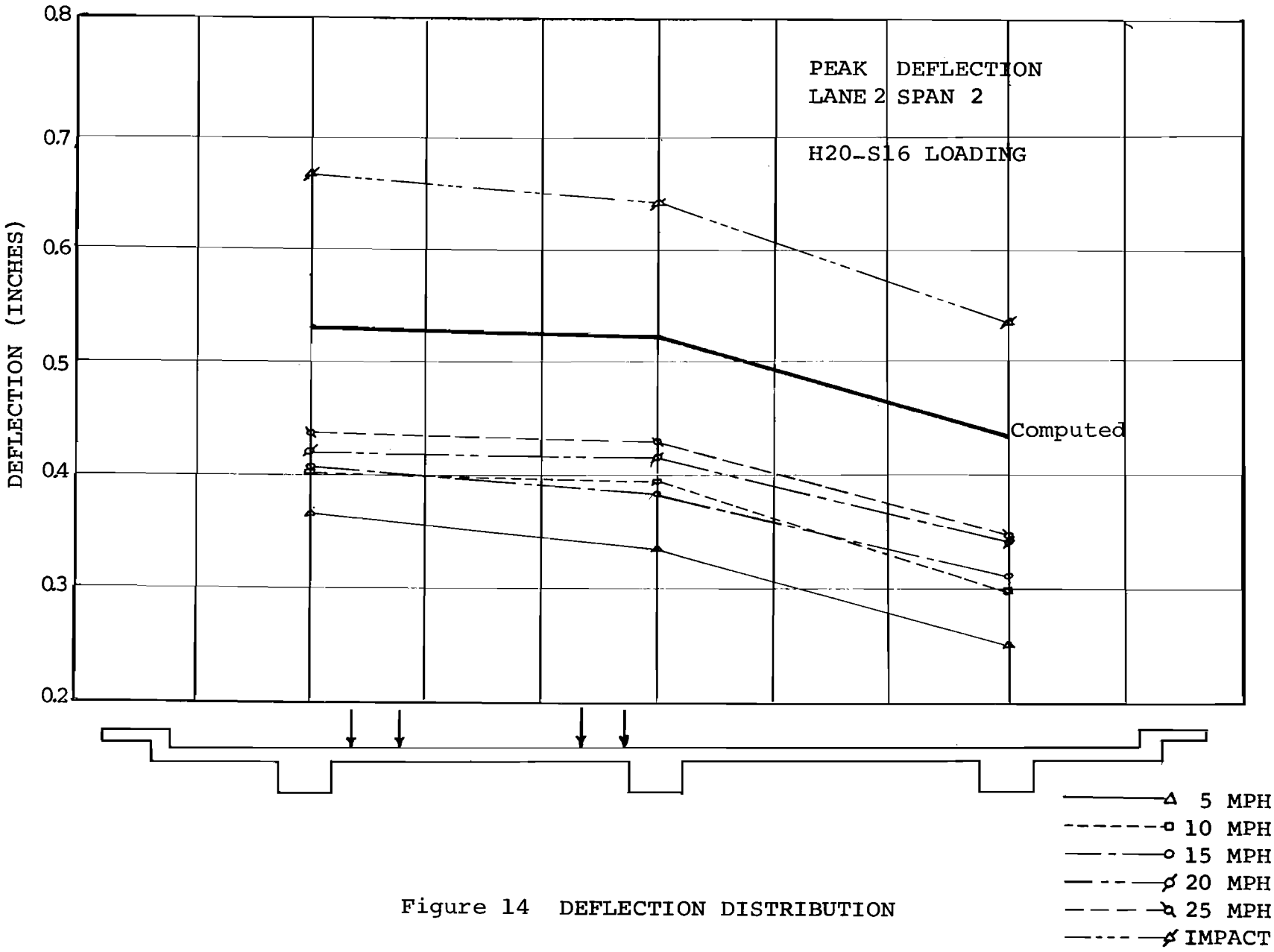

Figure 14 DEFLECTION DISTRIBUTION

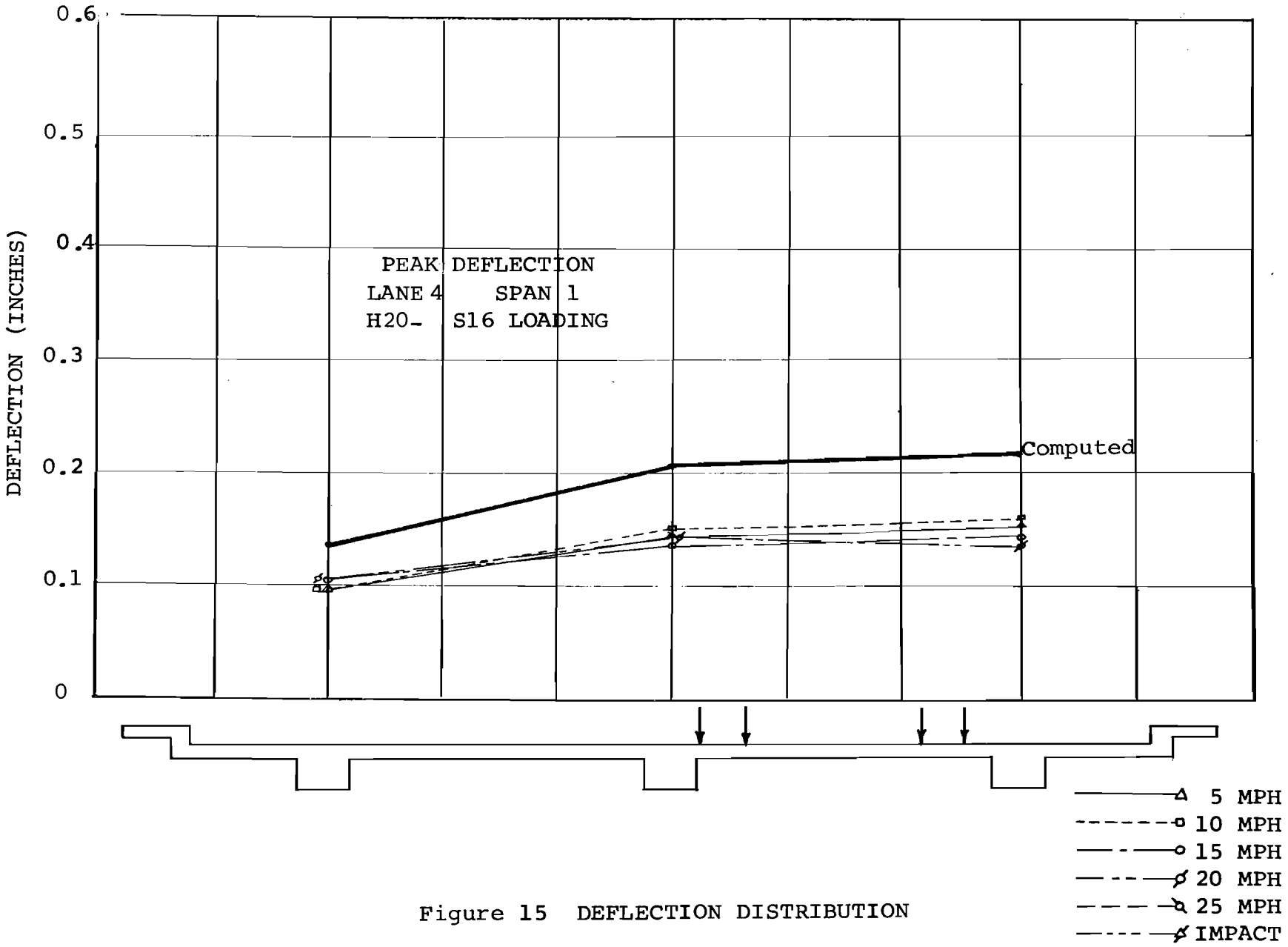

Figure 15 DEFLECTION DISTRIBUTION

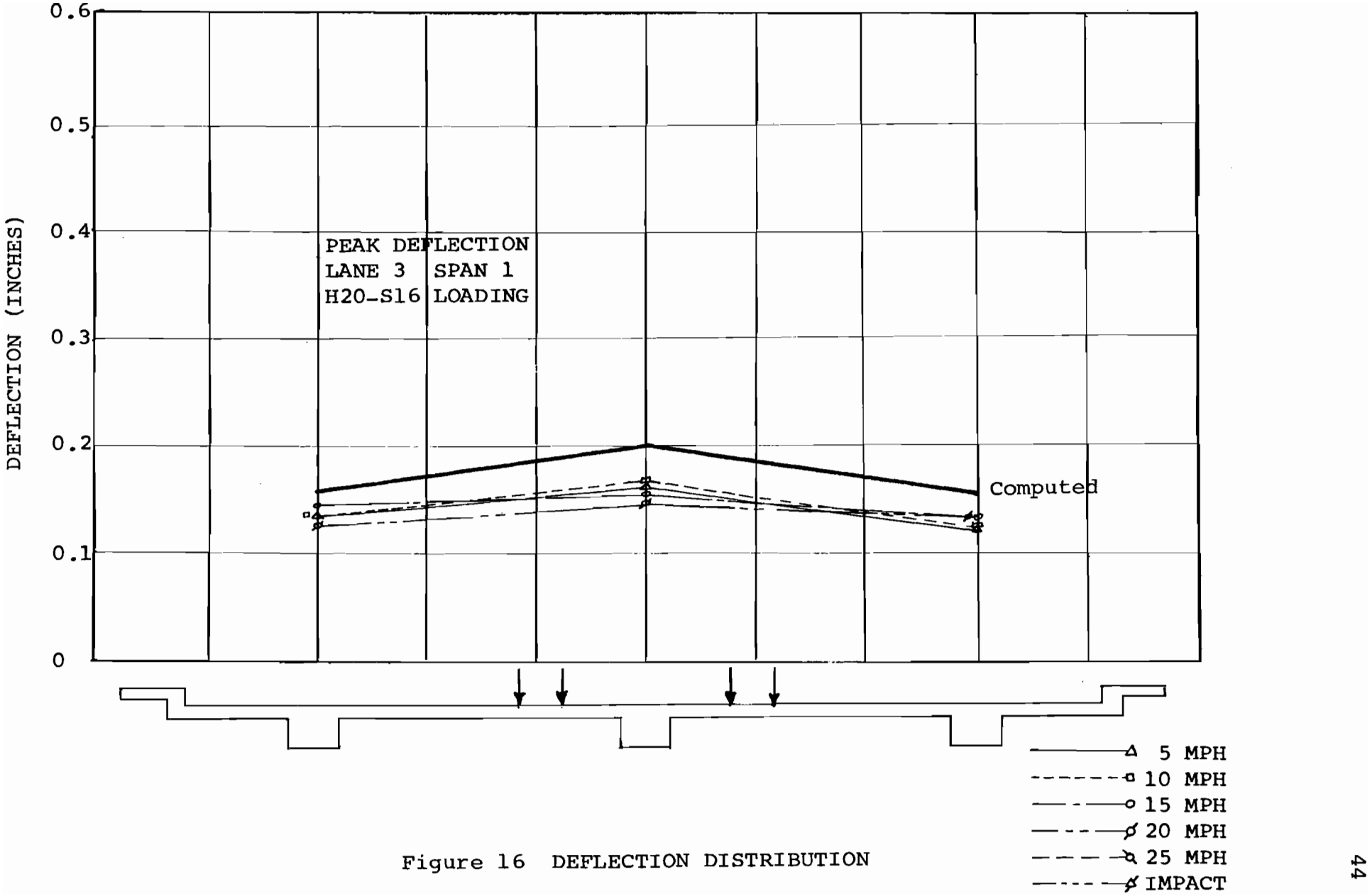

Figure 16 DEFLECTION DISTRIBUTION

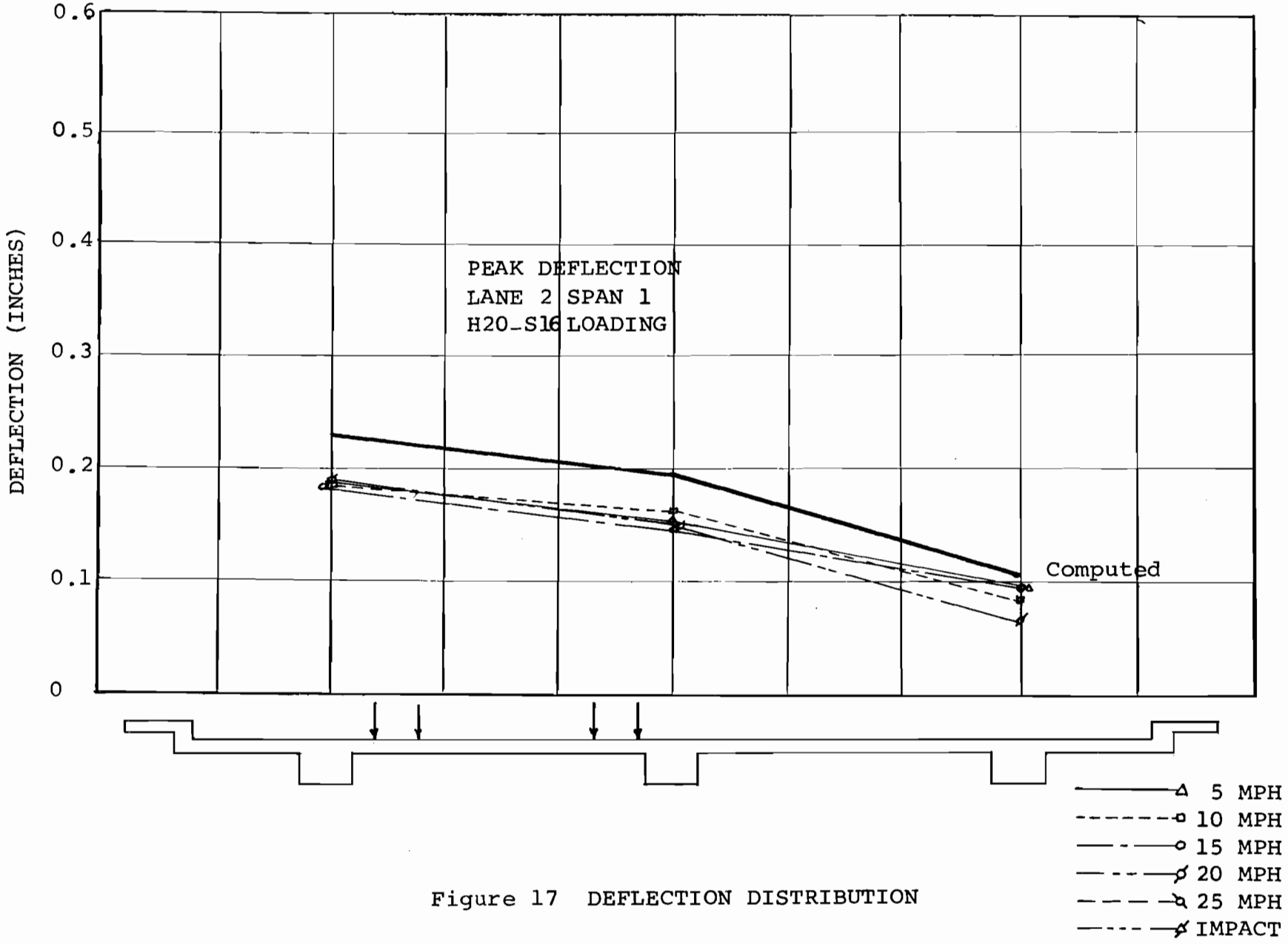

Figure 17 DEFLECTION DISTRIBUTION

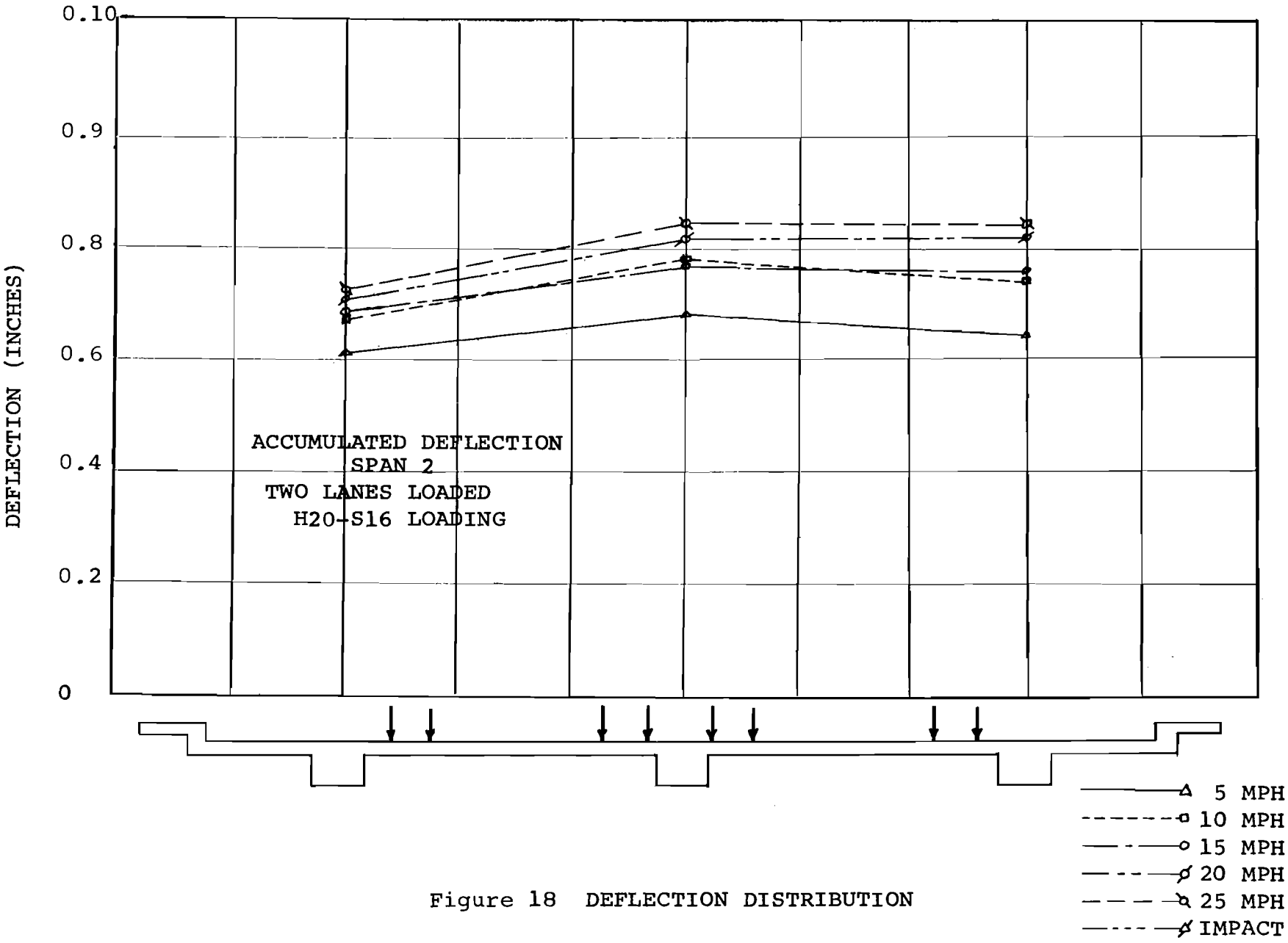

Figure 18 DEFLECTION DISTRIBUTION

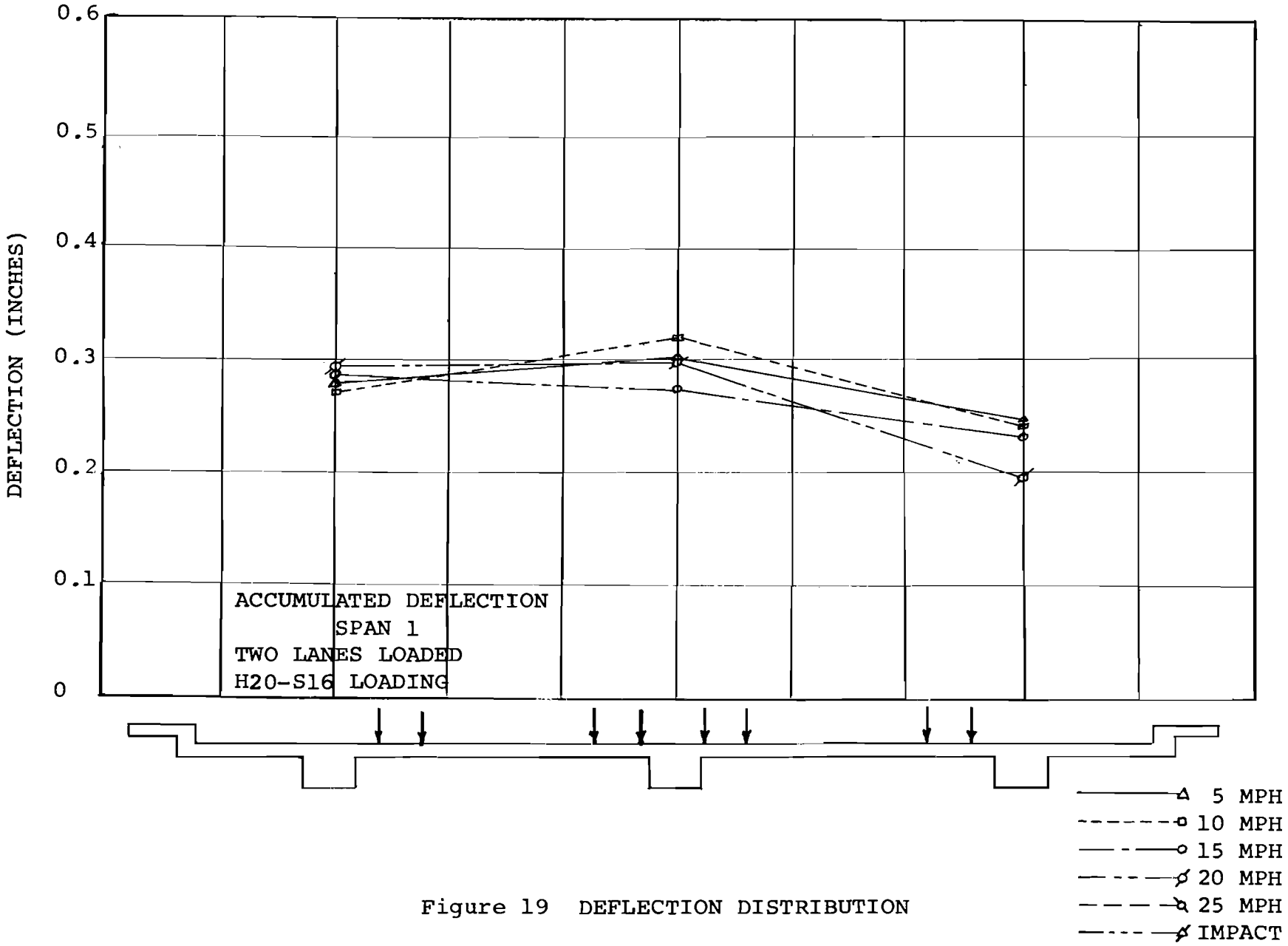

Figure 19 DEFLECTION DISTRIBUTION

TABLE 4

OBSERVED IMPACT FACTORS

Based on Reinforcing Steel Stresses

Gage Location	Lane #	Impact Factor *				Impact Boards	Remarks
		10 MPH	15 MPH	20 MPH	25 MPH		
Bottom of Girder Center of Span 3	2	1.00	1.02	1.00	1.19	-	H20-S16 Loadings
"	3	.98	-	.97	1.08	-	
"	4	.95	1.00	.99	1.22	-	
Top of Slab over Bent 3	2	-	1.40	-	-	-	
"	3	-	1.12	-	-	-	
"	4	-	1.09	-	-	-	
Top of Slab over Bent 4	2	1.26	-	-	-	-	
"	3	.91	-	-	-	-	
"	4	1.19	-	-	-	-	
Bottom of Girder 4/10 point Span 4	2	1.10	1.20	1.29	1.17	-	
"	3	.98	.95	.93	.83	-	
"	4	1.03	.91	.89	.89	-	
Top of Slab over Bent 2	2	1.13	1.19	1.00	1.16	1.86	Impact Boards at Center of Span 2
"	3	1.09	1.15	1.27	1.03	1.78	"
"	4	1.03	1.00	1.06	.97	1.66	"

*Impact Factor is defined as the ratio of stress at the speed indicated to the stress at crawl speed.

TABLE 5

OBSERVED IMPACT FACTORS

Based on Deflection of Center Girder

Point of Deflection	Lane#	Impact Factor* 10 MPH	15 MPH	20 MPH	25 MPH	Impact Boards	Remarks
Center of Span 3	2	1.21	1.18	1.47	1.20	-	H15-S12 Loading
"	3	1.40	1.12	1.22	1.17	-	↓
"	4	1.18	1.06	-	1.08	-	
Center of Span 4	2	1.08	1.13	1.05	1.10	-	
"	3	1.03	1.14	.96	1.03	-	
"	4	1.13	1.20	1.29	1.16	-	Last H15-S12 Loading
Center of Span 2	2	.87	.91	.93	1.11	-	H20-S16 Loading
"	3	1.01	.94	.98	1.08	-	↓
"	4	1.01	1.04	1.07	1.12	-	
Center of Span 1	2	1.12	1.16	1.17	1.27	-	
"	3	1.10	1.10	1.13	1.18	-	
"	4	1.14	1.08	-	1.17	-	
Center of Span 3	2	1.11	1.06	1.12	1.02	-	
"	3	1.07	1.07	1.08	1.05	-	
"	4	1.01	1.05	1.07	1.09	-	
Center of Span 2	2	1.17	1.13	1.24	1.28	1.90	Impact boards at Center of Span 2
"	3	1.15	1.14	1.17	1.13	1.84	"
"	4	1.13	1.13	1.17	1.20	1.82	"

*Impact Factor is defined as the ratio of deflection at the speed indicated to deflection at crawl speed.

TABLE 6

VIBRATION FREQUENCY OF TEST VEHICLE
DURING TEST RUNS (CPS)*

SPEED	LANE	RIGHT** FRONT	LEFT** FRONT	LEFT*** REAR	RIGHT*** REAR
10	2	3.33	3.00	3.00	3.00
	3	3.00	3.00	3.63	3.00
	4	3.63	3.63	3.63	3.33
15	2	3.33	3.33	3.00	2.31
	3	3.00	4.00	3.00	4.00
	4	2.35	3.07	2.97	3.00
20	2	2.80	2.80	2.85	2.82
	3	3.00	3.00	2.86	2.83
	4	2.85	2.87	2.75	2.75
25	2	3.60	3.50	4.33	4.00
	3	3.50	2.83	2.33	2.75
	4	5.00	4.50	4.25	4.25
10 I	2	4.50	4.50	3.25	3.25
	3	2.80	2.67	2.80	2.86
	4	3.00	3.00	3.00	3.00
15 I	3	3.33	4.00	3.00	3.00
	4	4.25	4.25	3.60	3.60

*ALL RESULTS ARE FOR H20-S16 LOADING. STRAIN GAGES MOUNTED ON AXLES WERE USED TO DETERMINE FREQUENCY OF VIBRATION.

**DRIVE AXLE

***REAR AXLE

TABLE 7

PEAK DOUBLE AMPLITUDES OF VIBRATION
MEASURED ON TRUCK AXLES

SPEED	LANE #	RIGHT DRIVE	LEFT DRIVE	RIGHT REAR	LEFT REAR
10	2	.695	.570	.720	.683
	3	.375	.294	.371	.445
	4	.385	.258	.327	.371
15	2	.660	.460	.445	.520
	3	.620	.553	.550	.653
	4	.525	.322	.415	.430
20	2	.826	.671	.950	.890
	3	.798	.478	.755	.830
	4	.600	.442	.542	.542
25	2	1.050	1.030	.745	.735
	3	.576	.555	.707	.560
	4	.620	.657	.595	.600
10I	2	1.196	1.126	1.290	1.208
	3	1.266	1.040	1.242	1.250
	4	1.180	.916	1.216	1.290
15I	3	1.512	1.196	1.452	1.368
	4	1.582	1.320	1.550	1.490

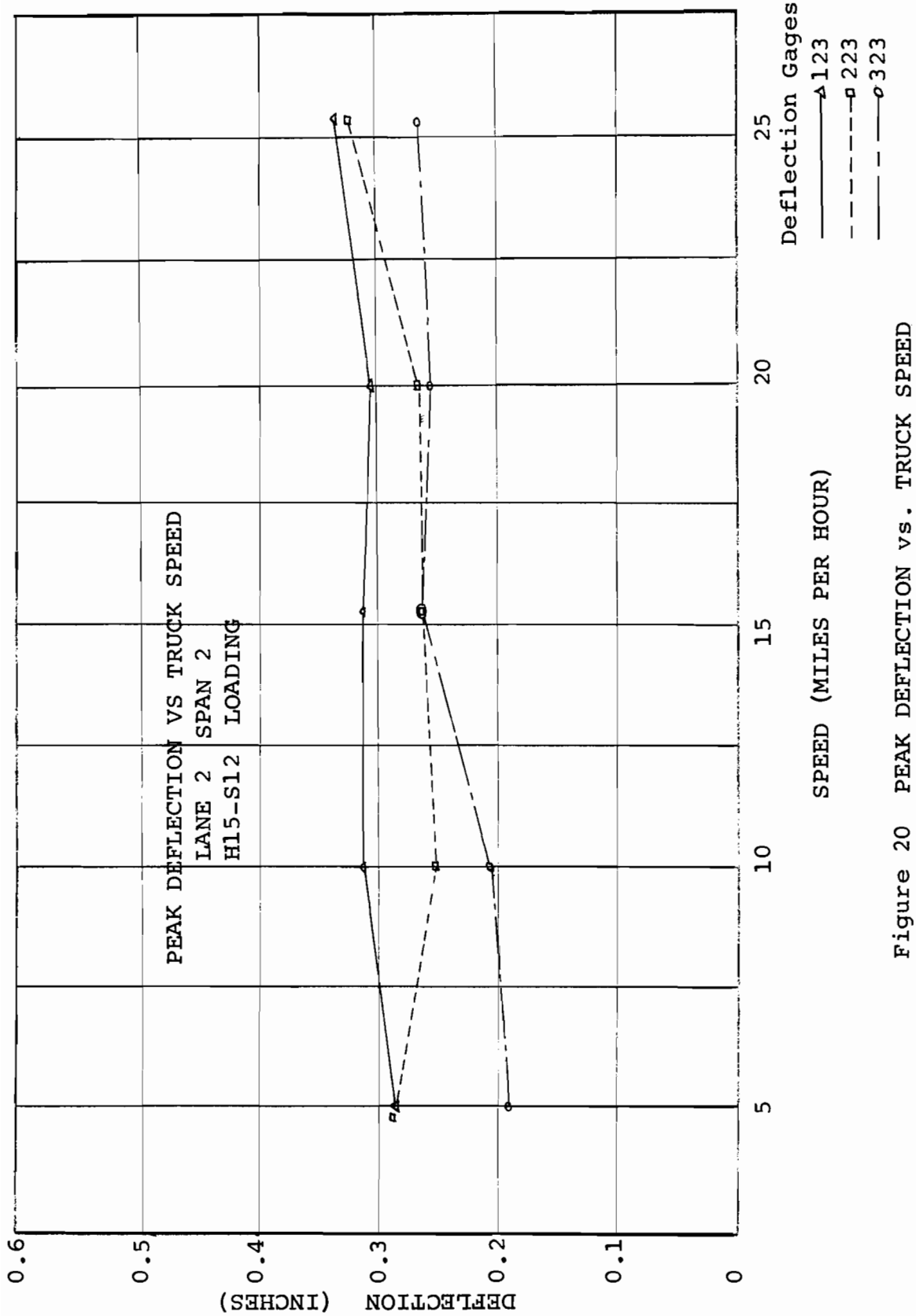

Figure 20 PEAK DEFLECTION vs. TRUCK SPEED

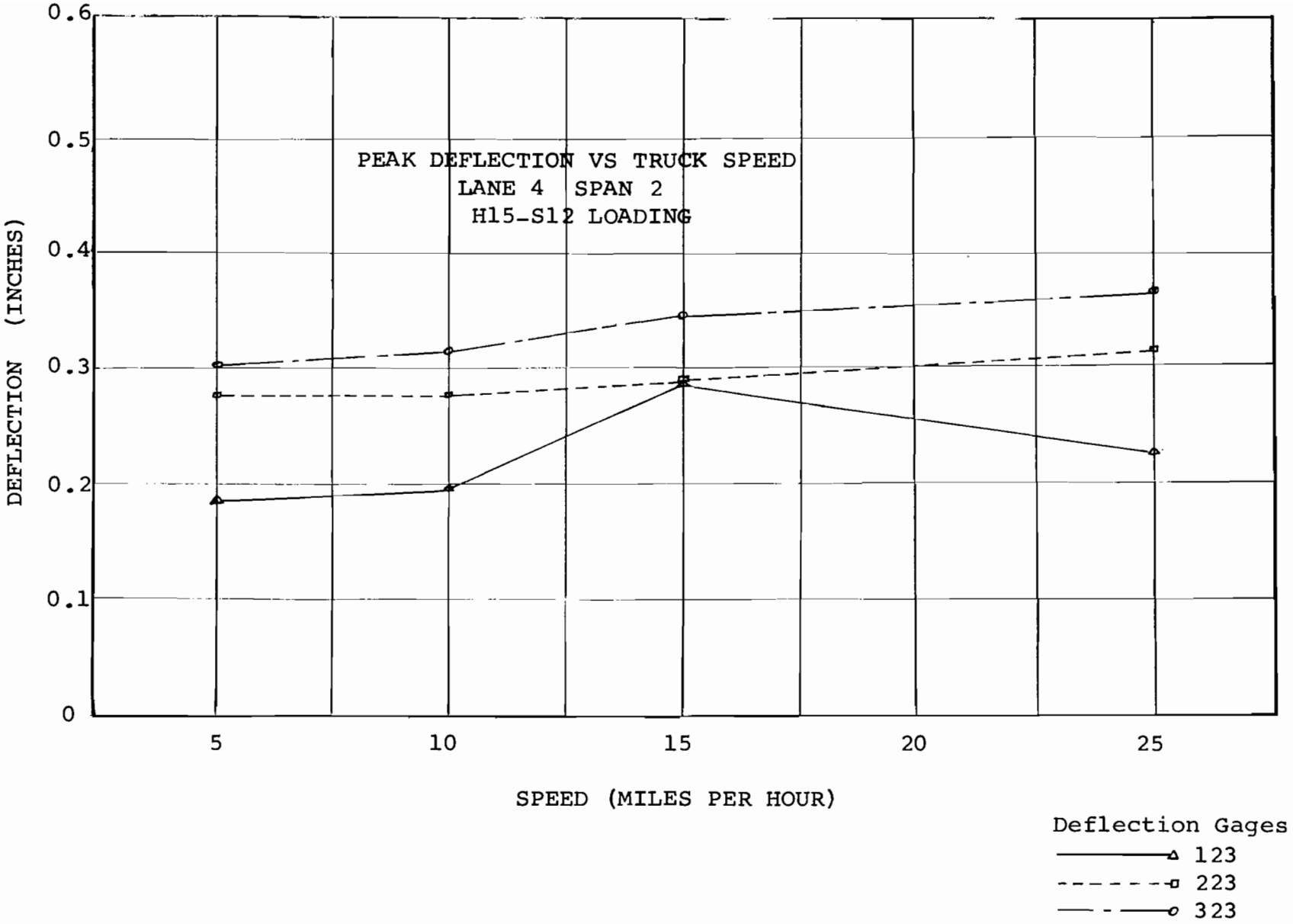

Figure 22 PEAK DEFLECTION vs. TRUCK SPEED

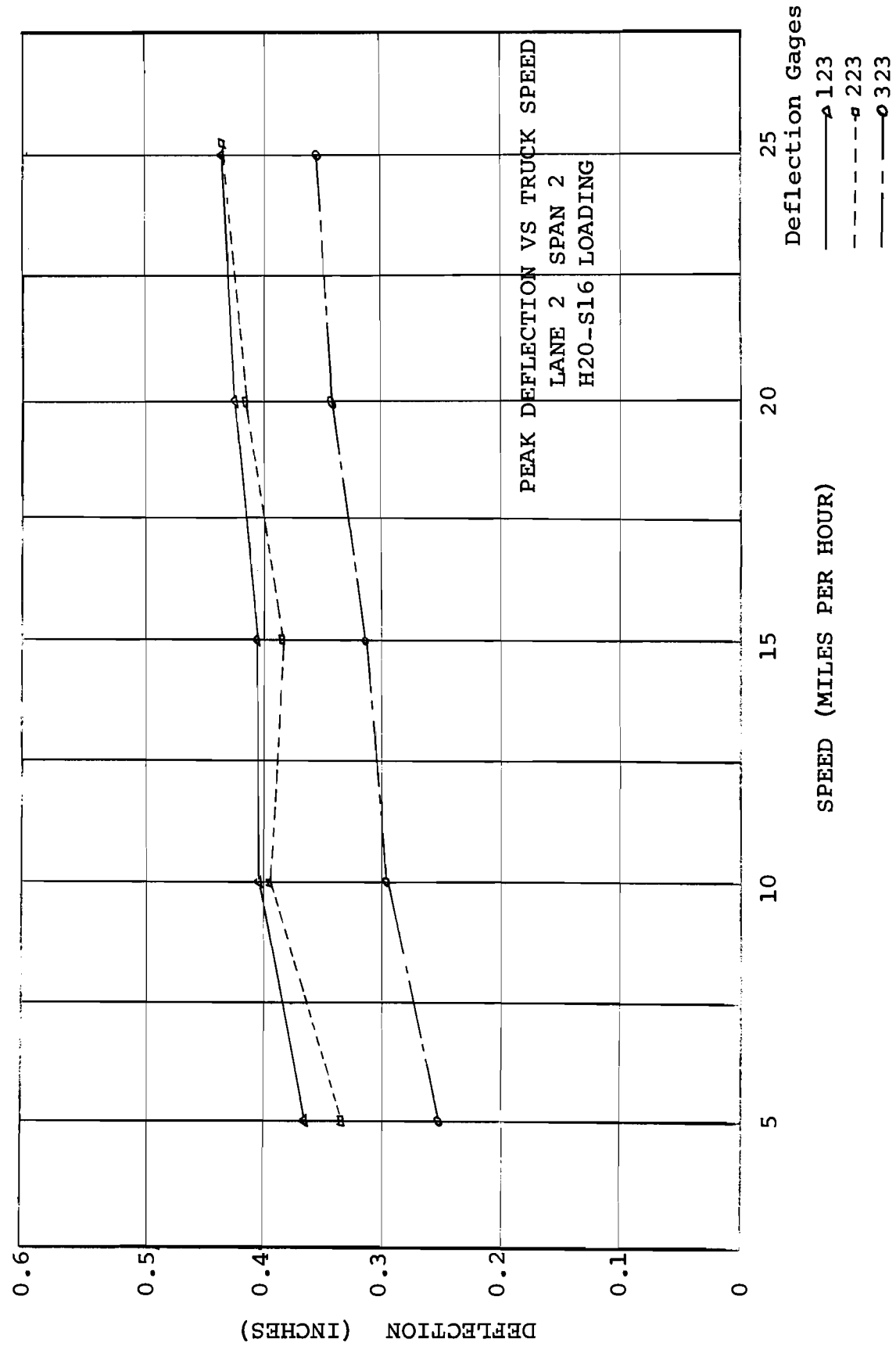

Figure 23 PEAK DEFLECTION vs. TRUCK SPEED

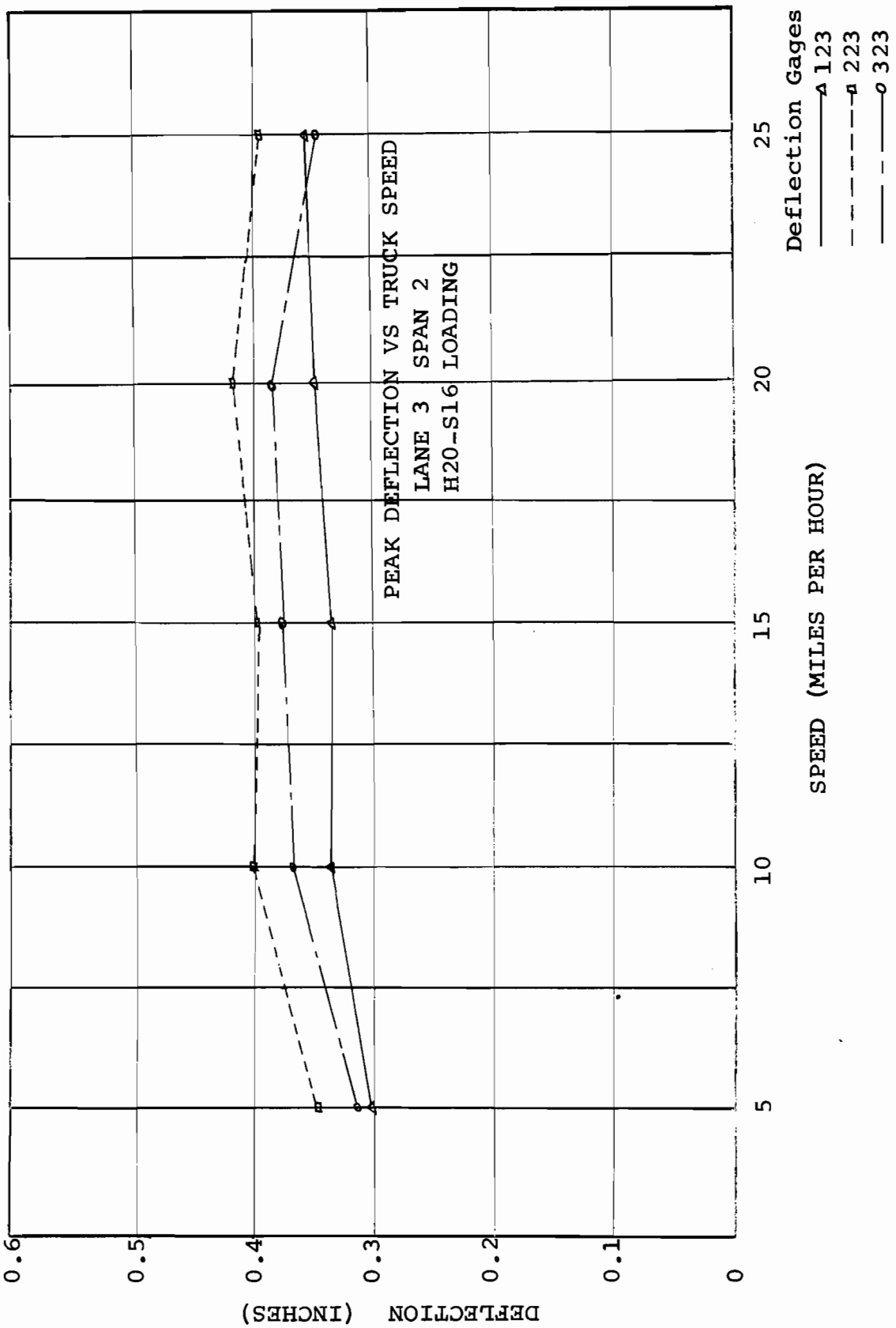

Figure 24 PEAK DEFLECTION vs. TRUCK SPEED

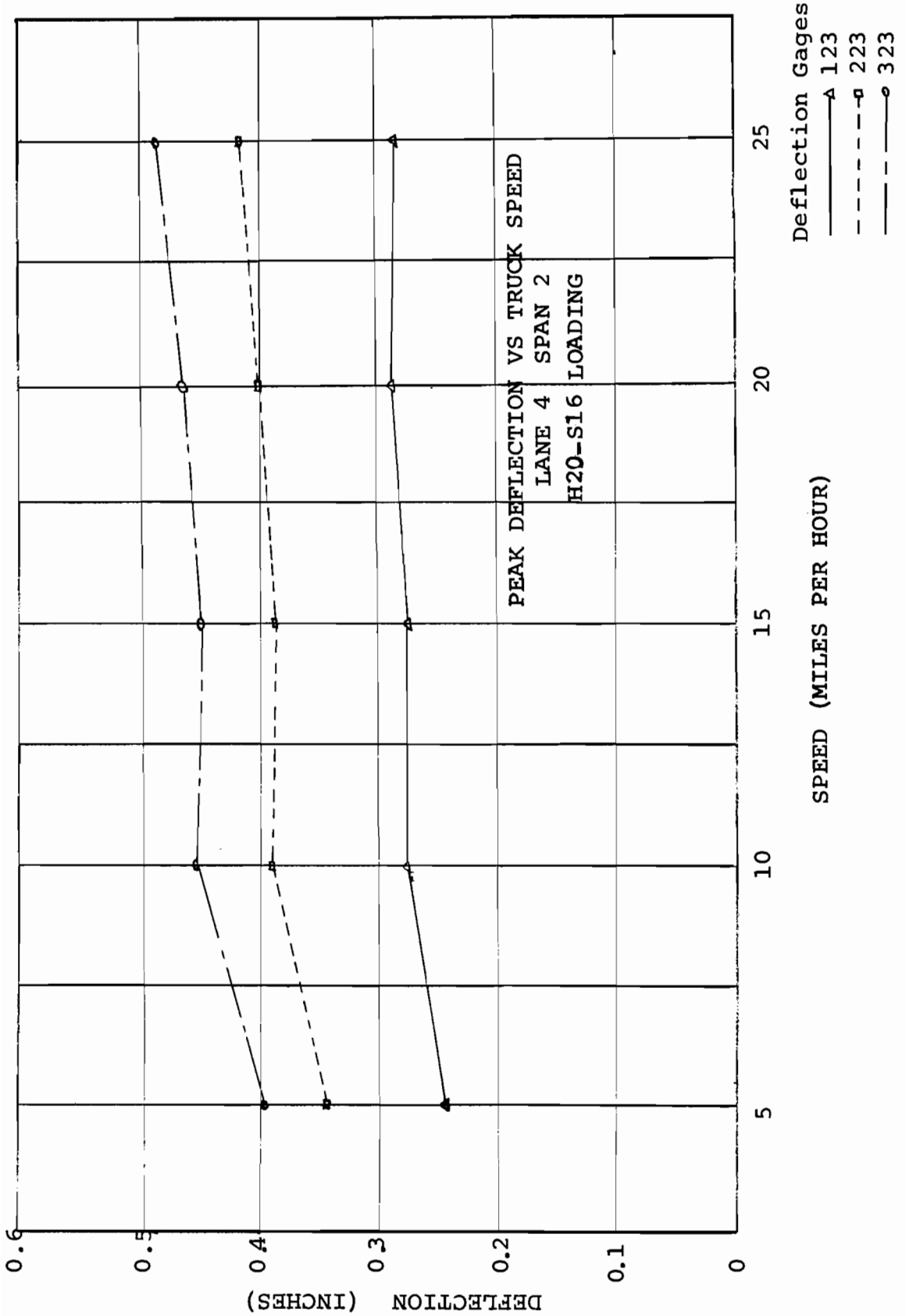

Figure 25 PEAK DEFLECTION vs. TRUCK SPEED

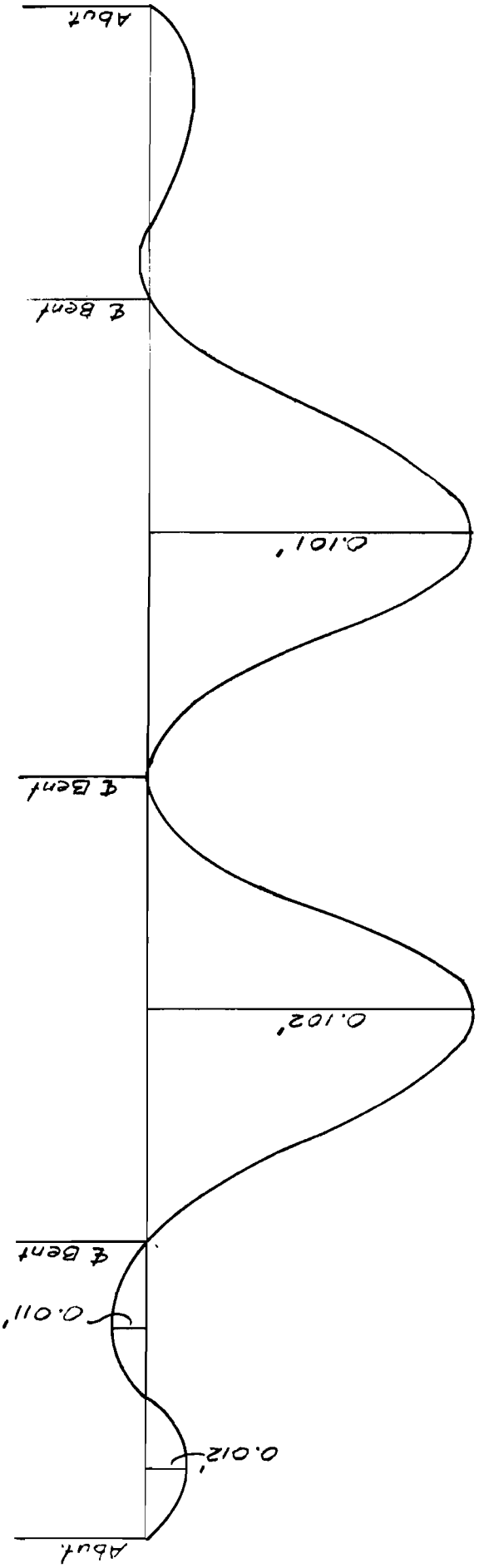

Figure 26 OBSERVED DEFLECTION DUE TO DEAD LOAD

After Form Release

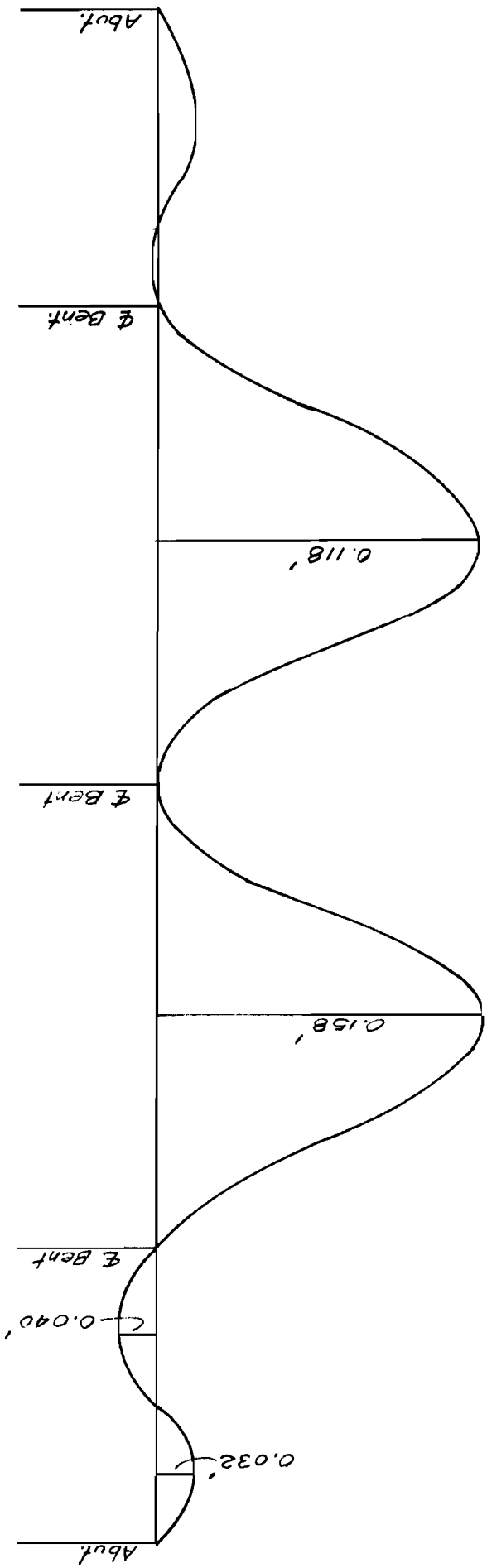

Figure 27 OBSERVED DEFLECTION DUE TO DEAD LOAD
CENTERLINE OF BRIDGE
FINAL READINGS (June 65)

TABLE 8

Forced Vibration Frequency of Bridge (CPS)

H 20 - S16 Loading

		Frequency (Cps)	
Speed	Lane	Span #1	Span #3
5 MPH	2	3.08	2.73
	3	2.67	2.86
	4	2.96	2.86
10 MPH	2	3.89	3.42
	3	3.57	3.57
	4	3.33	3.08
15 MPH	2	3.33	3.40
	3	2.67	2.50
	4	3.81	3.04
20 MPH	2	3.61	3.70
	3	2.50	3.81
	4	2.66	3.22
25 MPH	2	3.00	-
	3	2.67	-
	4	2.58	-

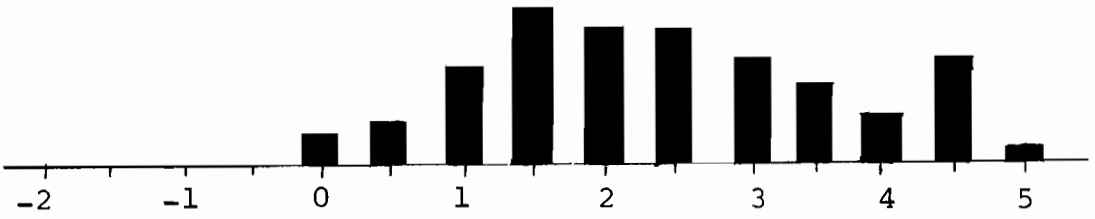

Observed Width-Theoretical Width

Watstein and Parsons' Equation

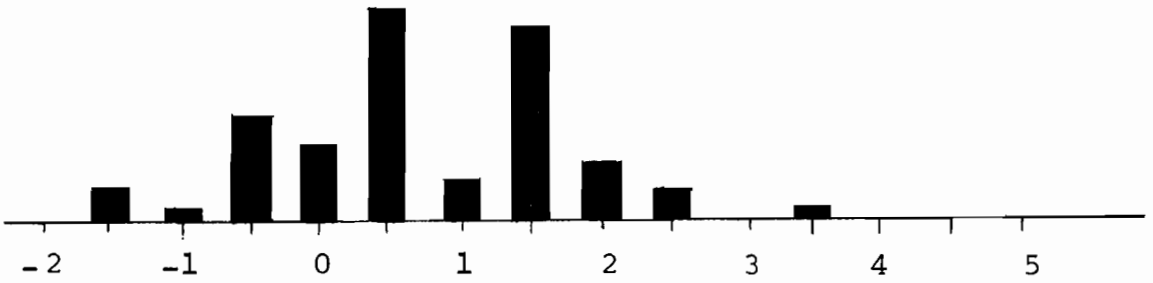

Observed Width-Theoretical Width

European Concrete Committee Equation

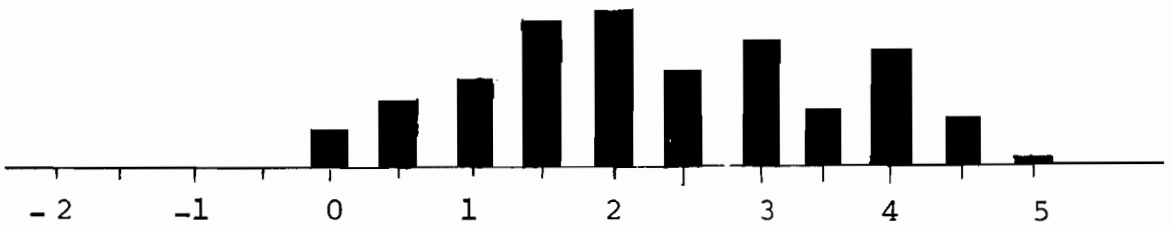

Occurrence Frequency

Observed Width-Theoretical Width

Johsson, Osterman and Wastlunds' Equation

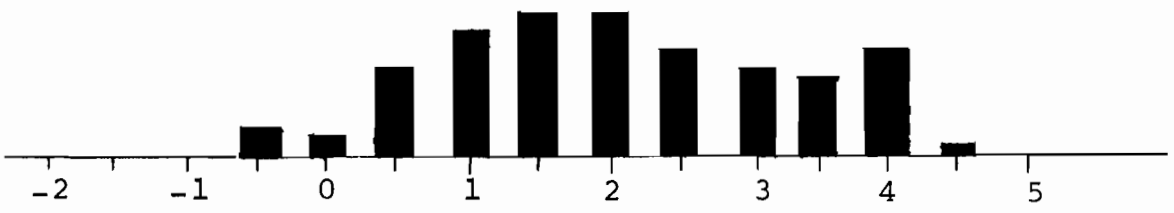

Observed Width-Theoretical Width

Kaar and Mattocks' Equation

Figure 28 DEVIATION FROM PREDICTED CRACK WIDTH

vs. OCCURRENCE FREQUENCY

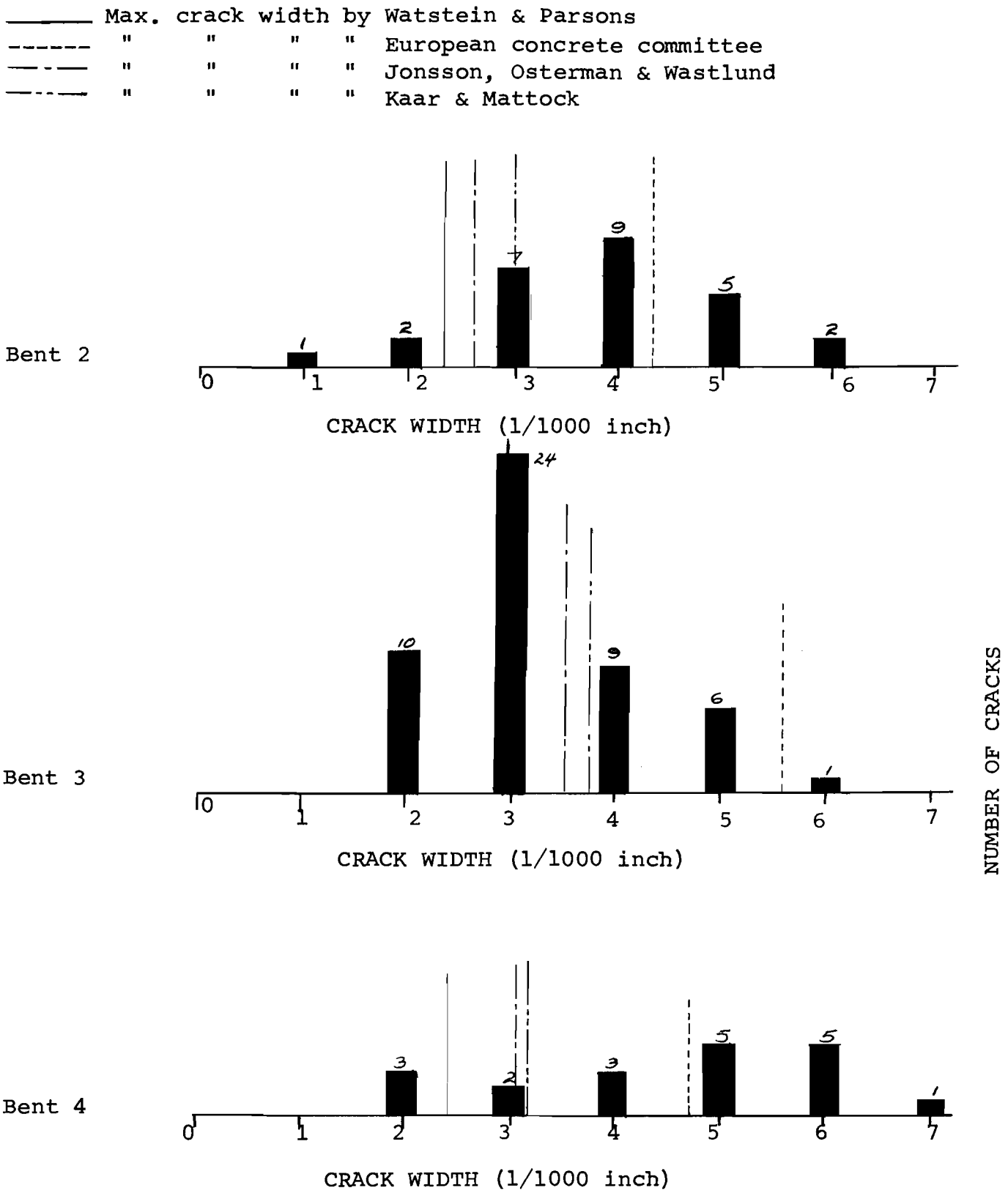

Figure 29 CRACK WIDTH VS OCCURRENCE FREQUENCY FOR EACH BENT (Before Traffic)

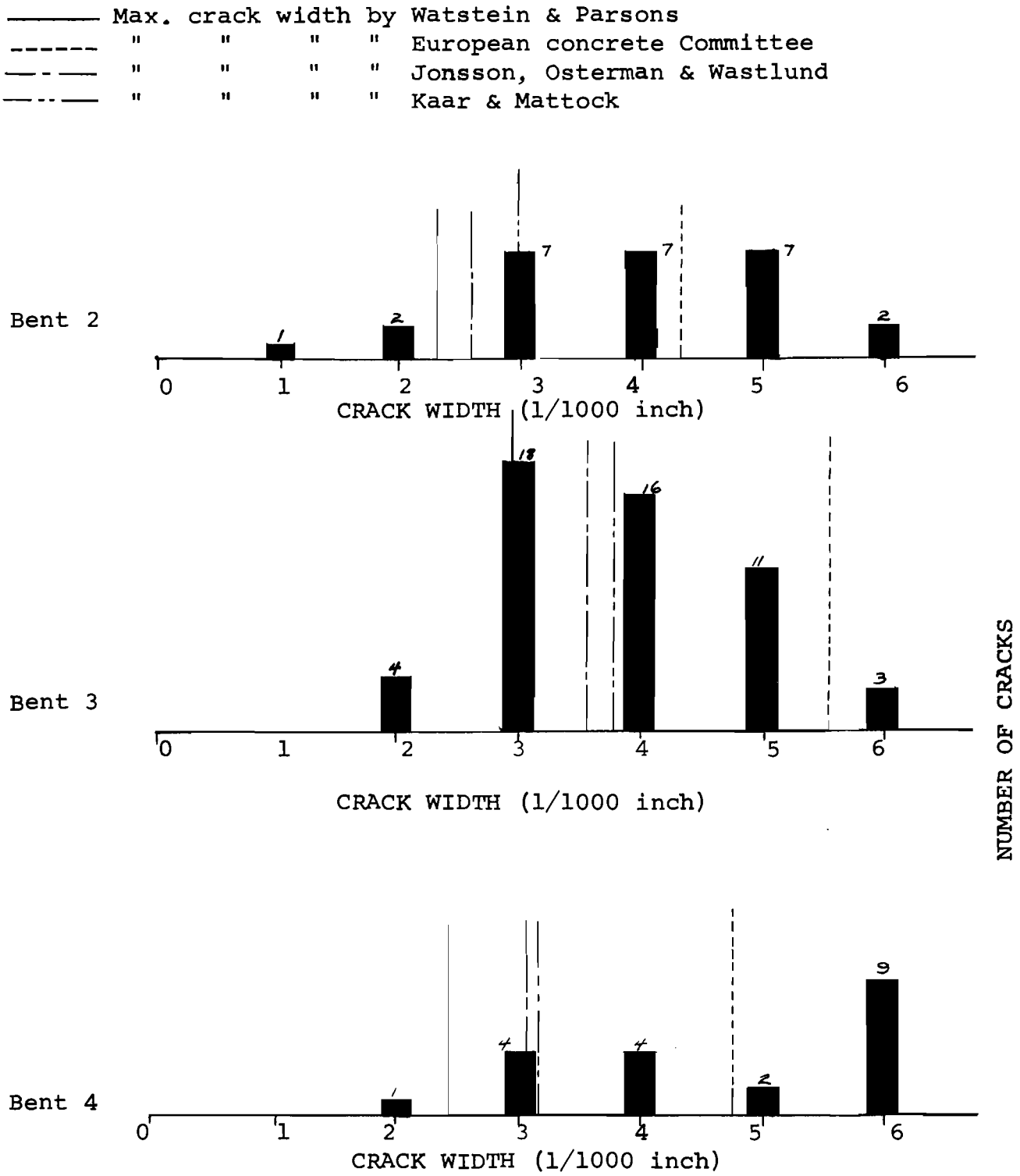

Figure 30 CRACK WIDTH VS OCCURRENCE FREQUENCY FOR EACH BENT (After Traffic)

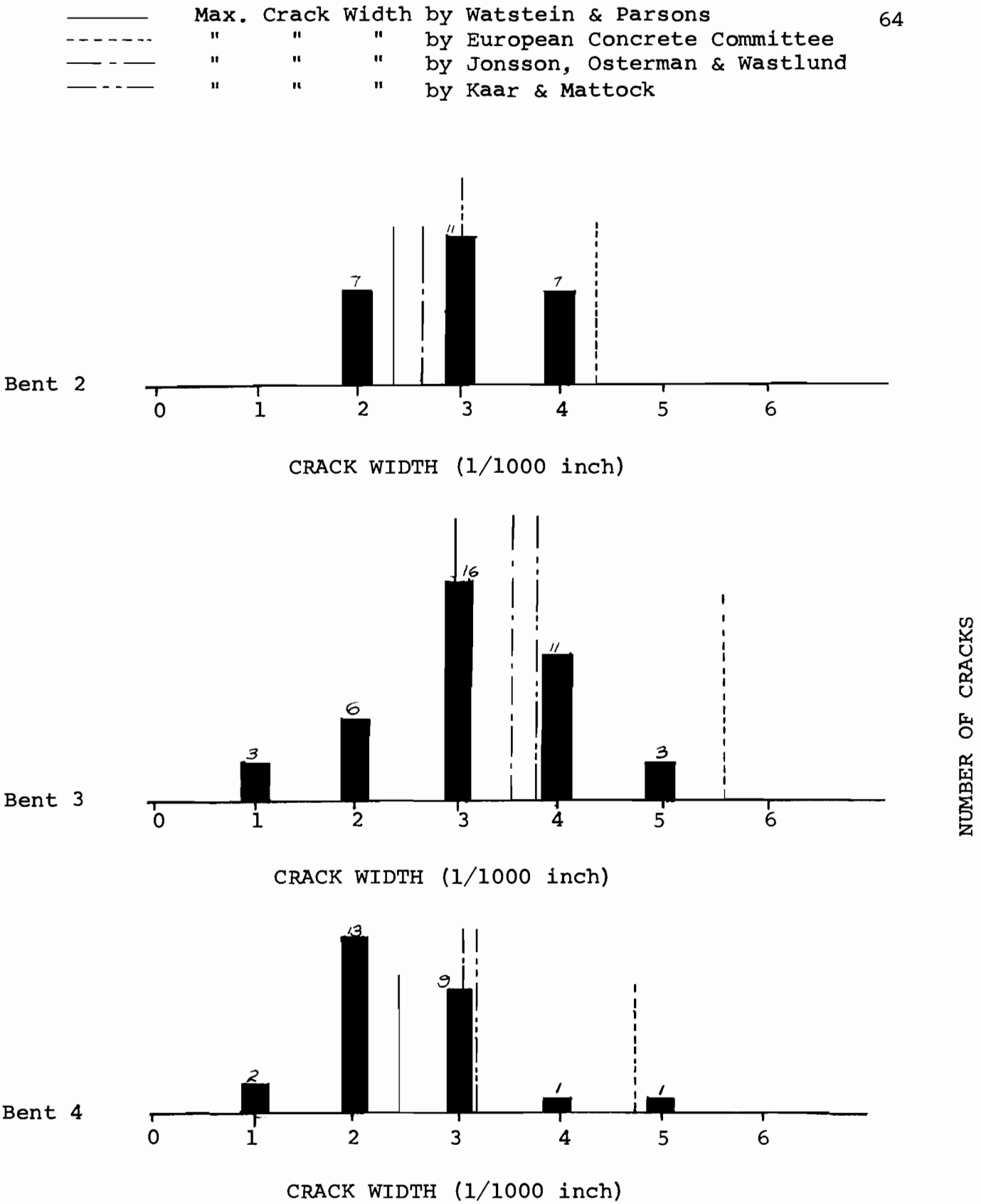

Figure 31 OBSERVED CRACK WIDTH VS OCCURRENCE FREQUENCY FOR EACH BENT (Final Readings)